This article was downloaded by:
On: *21 January 2011*
Access details: *Access Details: Free Access*
Publisher *Taylor & Francis*
Informa Ltd Registered in England and Wales Registered Number: 1072954 Registered office: Mortimer House, 37-41 Mortimer Street, London W1T 3JH, UK

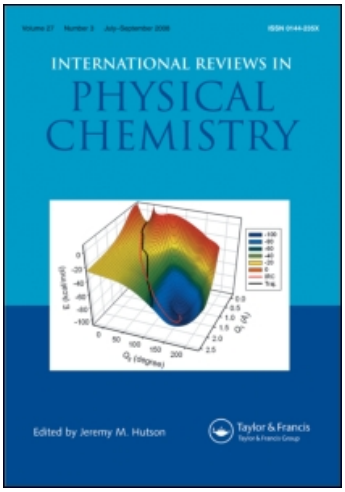

International Reviews in Physical Chemistry
Publication details, including instructions for authors and subscription information:
http://www.informaworld.com/smpp/title~content=t713724383

Quantum-chemical investigations of small molecular anions

P. Botschwina[a]; S. Seeger[a]; M. Mladenović[a]; B. Schulz[a]; M. Horn[a]; S. Schmatz[a]; J. Flügge[a]; R. Oswald[a]
[a] Institut für Physikalische Chemie, Universität Göttingen, Göttingen, Germany

To cite this Article Botschwina, P. , Seeger, S. , Mladenović, M. , Schulz, B. , Horn, M. , Schmatz, S. , Flügge, J. and Oswald, R.(1995) 'Quantum-chemical investigations of small molecular anions', International Reviews in Physical Chemistry, 14: 2, 169 — 204
To link to this Article: DOI: 10.1080/01442359509353308
URL: http://dx.doi.org/10.1080/01442359509353308

PLEASE SCROLL DOWN FOR ARTICLE

Full terms and conditions of use: http://www.informaworld.com/terms-and-conditions-of-access.pdf

This article may be used for research, teaching and private study purposes. Any substantial or systematic reproduction, re-distribution, re-selling, loan or sub-licensing, systematic supply or distribution in any form to anyone is expressly forbidden.

The publisher does not give any warranty express or implied or make any representation that the contents will be complete or accurate or up to date. The accuracy of any instructions, formulae and drug doses should be independently verified with primary sources. The publisher shall not be liable for any loss, actions, claims, proceedings, demand or costs or damages whatsoever or howsoever caused arising directly or indirectly in connection with or arising out of the use of this material.

INTERNATIONAL REVIEWS IN PHYSICAL CHEMISTRY, 1995, VOL. 14, NO. 2, 169–204

Quantum-chemical investigations of small molecular anions

by P. BOTSCHWINA, S. SEEGER, M. MLADENOVIĆ, B. SCHULZ, M. HORN, S. SCHMATZ, J. FLÜGGE and R. OSWALD

Institut für Physikalische Chemie, Universität Göttingen, Tammannstr. 6, D-37077 Göttingen, Germany

Dedicated to Dr Gerhard Herzberg on the occasion of his 90th birthday

Recent large-scale *ab initio* calculations for small negative molecular ions are reviewed. Accurate equilibrium geometries are established for several species like NH_2^-, HCC^-, NO_2^-, CH_2N^-, C_5^- and C_6^-. Predictions are made for various spectroscopic properties like vibrational frequencies, rotational constants and infrared intensities. The effects of a shallow energy minimum in the T-shaped configuration on the rovibrational term energies of HCC^- are investigated. The calculated vibrational structures of the photoelectron spectra of SiH_3^- and CH_2N^- are in very good agreement with the experiment. The present calculations support the assignment of an absorption observed at 608 nm in a neon matrix to the $\tilde{C}^2\Pi_g \leftarrow \tilde{X}^2\Pi_u$ transition of C_6^-. Electron affinities are obtained with an accuracy of 0·05 eV or better. Spectroscopic properties of intermediates in simple S_N2 reactions are calculated.

Downloaded At: 17:15 21 January 2011

1. Introduction

Although negative molecular ions are recognized to play an important role in various areas of chemistry and related disciplines, precise experimental information on the properties of the isolated species has been very difficult to obtain. Prior to 1983, rotationally resolved spectra had been reported only for two diatomic anions, C_2^- [1] and OH^- [2, 3]. Due to the development of new experimental techniques the situation changed in the middle of the eighties. Lineberger and coworkers were able to develop a variant of the laser electron detachment approach termed autodetachment spectroscopy and carried out the first high-resolution spectroscopic study of the open-shell anion NH^- [4]. The first polyatomic anion studied by this technique is HNO^- [5]. High-resolution autodetachment studies of excited electronic states of polyatomic species have been carried out for the acetaldehyde enolate anion, $C_2H_3O^-$ [6, 7], $C_2H_2OF^-$ [9], CH_2CN^- [8] and CH_2CC^- [10]. The necessary condition for this kind of spectroscopy to be successful is the existence of so-called dipole-bound states in which the excess electron is only slightly bound in the dipole field of the neutral core.

From 1985 on it has become possible to study the vibration–rotation spectra of molecular anions by means of direct laser absorption spectroscopy in electrical discharges. Special modulation techniques like velocity-modulation as introduced by the Saykally group at Berkeley [11] are required to achieve this goal. OH^- was the first diatomic species to be observed in this way [12, 13]. This was followed by the detection of infrared spectra of NH_2^- [14, 15], SH^- [16], N_3^- [17, 18], NCO^- [19], NCS^- [20], FHF^- [21, 22] and $ClHCl^-$ [23]. The assignment of 12 lines to rovibrational transitions within the ν_3 band of HCC^- [24] has been severely criticized on the basis of *ab initio* calculations [25, 26] and turned out to be incorrect [27].

Much of the relevant theoretical work on small molecular anions until 1989 has been authoritatively reviewed by Bates [28]. We feel that it is too early to give a similar

0144–235X/95 $10·00 © 1995 Taylor & Francis Ltd.

review on the more recent theoretical literature. Instead, we will present a more detailed overview about our theoretical work dealing with the calculation of spectroscopic properties of negative molecular ions and cluster ions most of which has not yet been published. The emphasis will be laid on closed-shell polyatomic anions although results for some diatomic anions and open-shell species will be reported as well.

After establishing the accuracy of current state-of-the-art *ab initio* calculations for experimentally rather well-known diatomic anions like OH^-, SH^-, NH^- and C_2^- we will make predictions for anions about which high-resolution gas-phase information is either absent or incomplete. Among these are CN^-, NH_2^-, NO_2^-, NCO^-, HO_2^-, HCC^-, SiH_3^-, CH_2N^-, HC_4^-, carbon cluster anions and the complexes $F^- \cdots CH_3F$, $Cl^- \cdots CH_3F$ and $Cl^- \cdots CH_3Cl$. We will report on accurate equilibrium structures, vibrational wavenumbers, rotational constants, vibration–rotation coupling constants, electric dipole moments, absolute intensities of vibrational transitions, photoelectron spectra, electron affinities and electronic excitation energies. The present predictions should be of help to experimentalists in the search for spectra of these species and their interpretation.

2. Methods of calculations

The common starting point of the *ab initio* calculation of spectroscopic properties is provided by the Born–Oppenheimer approximation. The approximate solution of the electronic Schrödinger equation at different nuclear configurations yields a potential for the motions of the nuclei. This is usually brought into suitable analytical form before the nuclear Schrödinger equation is solved, preferably by variational methods, thereby producing a set of rovibrational term energies and wavefunctions.

Ab initio quantum chemistry offers a variety of methods to solve approximately the electronic Schrödinger equation. In order to obtain high accuracy the inclusion of electron correlation effects is clearly mandatory. The most important methods currently available to achieve this goal are configuration interaction (CI), coupled cluster (CC) methods, (higher order) perturbation theory or density functional methods. While full-CI is still prohibitive for all but rather simple systems and relatively small basis sets, great advances have been made in multi configuration reference CI (MRCI) techniques [29]. For molecules with about 20 electrons reference spaces of several hundreds of configuration state functions (with orbitals determined in a preceding multi configuration self-consistent field (MCSCF) procedure, often of the complete active space (CAS) SCF type [30, 31]), can now be routinely performed even on rather inexpensive work-stations. Provided that one single reference configuration dominates the total wavefunction sufficiently strongly over the interesting region of the nuclear coordinate space, more economic single-reference coupled cluster methods can be used about equally well. In such cases, higher-order perturbation theory like Rayleigh–Schrödinger perturbation theory with energy partitioning due to Møller and Plesset at fourth order (MP4) [32] may also do a good job, but its reliability is sometimes hard to judge in advance. Among the current variants of CC (see [33] for a review), originally introduced by Coester, Kümmel and Čížek (see [34], [35] for a discussion of the origins), CCSD(T) is a particularly economic and powerful one (see, e.g., [36–39]). This acronym stands for a CC method involving single and double excitation operators (CCSD) plus a quasi-perturbative treatment of connected triple substitutions [40].

Open-shell coupled cluster theory based on a spin-restricted Hartree–Fock (RHF) reference wavefunction has been discussed by a number of authors [41–50]. We make use of the methods of Knowles *et al.* [49] and Deegan and Knowles [50] and will mostly

Downloaded At: 17:15 21 January 2011

present RCCSD(T) results, where the abbreviation 'R' stands for a partially spin-adapted formalism (see [49] for details).

We will also make use of more approximate methods like the coupled electron pair approximation (CEPA), introduced by Meyer [51, 52], and MP2 [53, 54]. The former may be regarded as an approximation to CCSD. In practical applications (see, e.g., [55, 56]) version 1 of CEPA (CEPA-1) mostly yields results intermediate between CCSD and CCSD(T). In a pioneering paper Rosmus and Meyer [57] have demonstrated its predictive power for diatomic hydride anions. Several applications to polyatomic anions have been reviewed in 1989 [26]. On the whole, the cost-effective CEPA-1 method works surprisingly well in comparison to more expensive and reliable CCSD(T). For all electronic structure calculations considered in this work we made use of the MOLPRO suite of programmes [58].

3. Diatomic anions—benchmark calculations and predictions

3.1. *OH^- and SH^-*

OH^- and SH^- are well-known through high-resolution infrared spectroscopy and are therefore well suited as benchmark cases to check the quality of the present calculations. For OH^-, three different basis sets are employed which have been recently proposed by Dunning and coworkers [59]. They are termed 'augmented correlation-consistent polarized valence triple-zeta' (avtz), 'augmented correlation-consistent polarized quadruple-zeta' (avqz) and 'augmented correlation-consistent polarized quintuple-zeta' (av5z) and comprise 69, 112 and 189 Gaussian type orbitals (cGTO; with real spherical harmonics for the angular parts) in the case of this molecule, respectively. For the largest basis set the g functions at the hydrogen atom were left out. In the calculations for SH^- the avqz and the av5z exclusive of g functions at hydrogen (193 cGTOs) were employed. The latter basis set has not yet been published, but is available in the MOLPRO basis set library. Valence electrons were correlated in both cases.

Downloaded At: 17:15 21 January 2011

A comparison of calculated and experimental values for some spectroscopic constants of OH^- and SH^- is made in table 1. The basis set dependence is shown for both species at the CCSD(T) level; for the largest basis sets we also quote the results obtained by SCF, MP2, CCSD and CEPA-1. On the CCSD(T) level of theory, increasing the basis set from avtz to avqz shortens the bond length by 0·0024 Å. Enlarging the basis further from avqz to av5z has very little effect on r_e. The CCSD(T) result for the bond length obtained with the latter basis set is in excellent agreement with experiment [13]. SCF, CCSD and CEPA-1 underestimate r_e by 0·022, 0·004 and 0·003 Å, respectively. MP2 is very close to experiment, but this appears to be fortuitous.

The wavenumber of the fundamental vibration (ν_{0-1}) obtained with the CCSD(T) method differs from experiment by only 7·0 cm^{-1}. CEPA-1 performs almost equally well while CCSD yields too large a value by 59·6 cm^{-1}. MP2 overestimates the experimental result by as much as 118 cm^{-1} or 3·3%.

The CCSD(T) value for the vibration–rotation coupling constant also agrees almost perfectly with the experimental value. Throughout this work, the theoretical values for α_e were obtained by taking three vibrational levels ($v = 0$, 1 and 2) into account and making use of the formula $\alpha_e \approx B_0 - 3B_1 + 2B_2$.

Mainly due to the neglect of core and core-valence correlation effects the CCSD(T) equilibrium bond length for SH^- is too long by 0·0022 Å (193 cGTO basis). The CCSD(T) value for ν_{0-1} differs from the experimental one by only 1·3 cm^{-1}. MP2 yields

Table 1. Calculated and experimental spectroscopic constants of OH^- and SH^-.

Ion	Method	Basis set	Ref.	r_e(Å)	ω_e(cm^{-1})	ν_{0-1}(cm^{-1})	α_e(cm^{-1})
OH^-	PNO-CEPA	53 cGTOs	[57]	0·961	3809	3621	0·766
	MR-CI	73 cGTOs	[127]	0·967	3731	3547	0·791
	CCSD(T)	69 cGTOs	this work	0·9678	3723·5	3541·3	0·781
	CCSD(T)	112 cGTOs	this work	0·9654	3741·5	3556·2	0·772
	SCF	189 cGTOs	this work	0·9421	4070·7	4885·7	0·743
	MP2	189 cGTOs	this work	0·9646	3816·3	3673·6	0·680
	CCSD	189 cGTOs	this work	0·9608	3801·2	3615·4	0·770
	CEPA-1	189 cGTOs	this work	0·9623	3764·0	3566·1	0·793
	CCSD(T)	189 cGTOs	this work	0·9649	3747·7	3562·6	0·771
	exp.		[13]	0·9643	3738·4	3555·6	0·772
SH	PNO-CEPA	53 cGTOs	[57]	1·348	2642	2538	0·300
	CEPA-1	84 cGTOs	[60]	1·346	2637	2533	0·298
	CCSD(T)	116 cGTOs	this work	1·3468	2645·0	2541·8	0·299
	SCF	193 cGTOs	this work	1·3328	2781·5	2687·1	0·271
	MP2	193 cGTOs	this work	1·3391	2723·6	2631·2	0·273
	CCSD	193 cGTOs	this work	1·3426	2672·7	2568·5	0·291
	CEPA-1	193 cGTOs	this work	1·3443	2653·4	2547·3	0·296
	CCSD(T)	193 cGTOs	this work	1·3455	2648·7	2544·6	0·294
	exp.		[19]	1·3433	2647·1	2540·5	0·2968

Downloaded At: 17:15 21 January 2011

an overestimate by 76·5 cm^{-1} or 3·6%. CEPA-1 (0·3% error) performs very well and CCSD (1·1% error) yields a significantly worse result. The vibration–rotation coupling constant is reproduced very well both by the previous CEPA calculations [57, 60] as well as the present CCSD, CEPA-1 and CCSD(T) calculations.

3.2. *NH^-*

The first high-resolution infrared spectrum of any negative molecular ion was recorded by Neumark *et al.* [61]. They investigated the $v = 1 \leftarrow 0$ band of NH^- ($X^2\Pi$) by means of a coaxial ion-beam laser-beam spectrometer. More recent work was published by Farley and coworkers [62–64].

High-quality *ab initio* calculations for NH^- have been published by Rosmus and Meyer [57] and by Mänz *et al.* [65]. We have carried out calculations by both CASSCF and internally contracted MRCI methods using a large basis set of 189 cGTOs (av5z exclusive of g functions at hydrogen). Active orbitals in the CASSCF calculations are 2σ–4σ, $1\pi_x$–$2\pi_x$ and $1\pi_y$–$2\pi_y$. The nitrogen core orbital (1σ) is left doubly occupied, but it is optimized. The CASSCF ansatz comprises 196 configuration state functions (CSFs) which serve as reference configurations in subsequent MRCI, in which all electrons are correlated.

Calculated and experimental spectroscopic constants for NH^- are compared in table 2. MRCI yields a wavenumber of 3022·4 cm^{-1} for the fundamental vibrational transition ν_{0-1}, which deviates from experiment by only 2·0 cm^{-1}. A larger difference of 10 cm^{-1} is found for ω_e, but again, since only one band could be observed, the experimental value may be less accurate than indicated by the standard deviation of the fit. The experimental α_e value of 0·704 cm^{-1} [63] was approximated as $\alpha_e \approx B_0 - B_1$ and thereby neglects the effects of quadratic and higher terms in the vibrational quantum number, the former of which are included in the determination of the present α_e values. Our $B_0 - B_1$ differences are 0·696 cm^{-1} (CASSCF), 0·701 cm^{-1} (MRCI) and 0·706 cm^{-1} (MRCI + D), the latter two being in excellent agreement with experiment.

Table 2. Calculated and experimental spectroscopic constants of NH^- ($X^2\Pi$).

Method	Basis set	Ref.	r_e(Å)	ω_e(cm^{-1})	ν_{0-1}(cm^{-1})	α_e(cm^{-1})
PNO-CEPA	57 cGTOs	[57]	1·039	3226	3056	0·691
MRCI (11)	79 cGTOs	[65]	1·045	3173	2979†	0·876
CEPA-1	85 cGTOs	[65]	1·043	3155	2995†	0·731
CASSCF	189 cGTOs	this work	1·0539	3077·0	2908·1	0·740
MRCI (196)	189 cGTOs	this work	1·0396	3181·5	3022·4	0·664
MRCI (196) + D‡	189 cGTOs	this work	1·0394	3182·5	3023·0	0·659
exp.		[63,64]	1·0399	3191·5 ± 2·1	3020·4	0·706§

† Calculated as $\nu_{0-1} \approx \omega_e - 2\omega_e x_e$ from the data of [65].
‡ Including multireference Davidson's correction.
§ Calculated approximately as $B_0 - B_1$; see also the text.

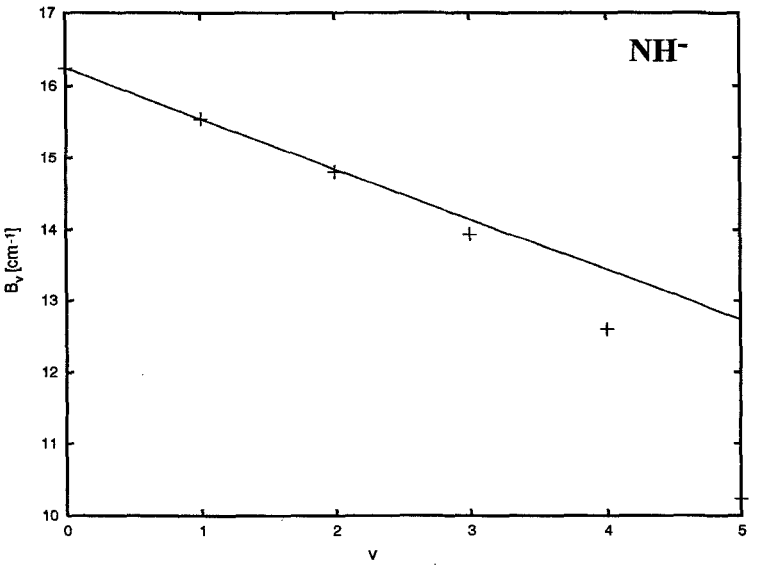

Figure 1. Dependence of the rotational constant B_v on the vibrational quantum number v for NH^-.

The importance of higher terms for the calculation of α_e is shown in figure 1, where the deviation of B_v from linearity is clearly obvious. Since the vibrational states with $v > 1$ are subject to autoionization the experimentalist is unable to see this behaviour. The MRCI values for the quartic centrifugal distortion constants in the two lowest vibrational states are $D_0 = 1{\cdot}769 \times 10^{-3}\,cm^{-1}$ and $D_1 = 1{\cdot}740 \times 10^{-3}\,cm^{-1}$. They differ from the experimental values [63] by less than 1%. Even the corresponding sextic terms, $H_0 = 1{\cdot}2 \times 10^{-7}\,cm^{-1}$ and $H_1 = 1{\cdot}0 \times 10^{-7}\,cm^{-1}$, are in reasonable agreement with the experimental values of $1{\cdot}8 \times 10^{-7}\,cm^{-1}$ and $1{\cdot}6 \times 10^{-7}\,cm^{-1}$.

3.3. C_2^- ($X^2\Sigma_g^+$, $A^2\Pi_u$ *and* $B^2\Sigma_u^+$)

Calculated and experimental spectroscopic constants of the three lowest doublet states of C_2^- are listed in table 3. In the present RCCSD(T) calculations (all electrons correlated) a basis set of 170 cGTOs has been employed (14s,9p,5d,2f,1g contracted to [10,9,5,2,1]), which corresponds to the 255 cGTO basis employed in our previous

Downloaded At: 17:15 21 January 2011

Table 3. Spectroscopic constants for C_2^-.

State	Method	R_e (Å)	ω_e (cm^{-1})	ν_{0-1} (cm^{-1})	α_e (cm^{-1})	T_e (ev)
$X^2\Sigma_g^+$	MRD-CI [134]	1·278	1880			0
	MRCI [131]	1·276	1780	1756	0·016	0
	CCSD(T)† [133]	1·267	1799			0
	RCCSD(T)	1·2686	1785·4	1762·3	0·0164	0
	MRCI	1·2704	1779·5	1756·3	0·0164	0
	MRCI + D	1·2704	1776·5	1753·1	0·0165	0
	MR-ACPF	1·2700	1777·2	1753·8	0·0165	0
	exp. [132]	1·2683	1781·2	1757·9	0·0165	0
$A^2\Pi_u$	MRD-CI [134]	1·318	1653			0·40
	MRCI [131]	1·318	1646	1624	0·016	0·44
	CCSD(T)† [133]	1·307	1676			0·553
	RCCSD(T)	1·3076	1673·2	1651·1	0·0160	0·473
	MRCI	1·3086	1668·5	1646·2	0·0160	0·494
	MRCI + D	1·3090	1664·5	1642·2	0·0161	0·482
	MR-ACPF	1·3090	1664·7	1642·9	0·0161	0·488
	exp. [132]	1·3077	1666·4	1644·8	0·0160	0·494
$B^2\Sigma_u^+$	MRD-CI [134]	1·222	1968			2·33
	MRCI [131]	1·231	1983	1951	0·017	2·35
	CCSD(T)† [133]	1·222	2013			2·453
	RCCSD(T)	1·2192	2031·0	2007·3	0·0160	2·366
	MRCI	1·2254	1967·9	1937·6	0·0179	2·346
	MRCI + D	1·2256	1963·6	1933·0	0·0180	2·322
	MR-ACPF	1·2252	1964·5	1934·2	0·0180	2·291
	exp. [135]	1·2234	1969·5	1939·3	0·0189	2·2802

† Based on an unrestricted Hartree–Fock determinant. Basis: cc–pVQZ.

Downloaded At: 17:15 21 January 2011

calculations for C_3 [66] and we refer to that work for details. The values for the electronic ground state and the first excited state are compared with the experimental data of Rehfuss *et al.* [132], those for the second excited state with results obtained by Mead *et al.* [135].

For the electronic ground state our results compare very well with those of Watts and Bartlett [133], who used Dunning's cc–pVQZ basis set [82] and an open-shell CCSD(T) formalism based upon a UHF reference wave function. The present RCCSD(T) calculations overestimate R_e *and* ν_{0-1} by only 0·0003 Å and 4·4 cm^{-1}, respectively. Similar results are observed for the first excited state.

For the second excited state, $B^2\Sigma_u^+$, the multi-reference methods perform considerably better than the coupled cluster methods. In particular, the calculated ν_{0-1} values are within 6 cm^{-1} of experiment while the present RCCSD(T) calculations produce a value which is too large by as much as 68 cm^{-1}.

For the equilibrium excitation energies (T_e) the present MRCI and MR-ACPF calculations represent definitive improvement over the previous theoretical work. The latter differ from experiment by only − 0·006 eV ($A^2\Pi_u$) and 0·011 eV ($B^2\Sigma_u^+$). Again, RCCSD(T) does a better job for the $A^2\Pi_u$ state (error: 0·021 eV) compared with the $B^2\Sigma_u^+$ state (error: 0·086 eV).

3.4. *CN^-*

Despite several attempts the high-resolution infrared spectrum of CN^- could not yet be analysed. Previous *ab initio* predictions [67, 68] place the origin of the $1 \leftarrow 0$ rovibrational band at 2052(6) and 2055(6) cm^{-1}, respectively, and both yield 1·177 Å for the equilibrium bond length. In this work, the much larger avqz basis (160 cGTO)

Table 4. Calculated spectroscopic constants of CN^-.

Method	Basis set	R_e(Å)	ω_e(cm^{-1})	ν_{0-1}(cm^{-1})	α_e(MHz)
CEPA-1†	60 cGTOs	1·1768	2105·6	2081·4	486
CEPA-1†	92 cGTOs	1·1804	2079·9	2055·6	492
MP4SDQ‡	66 cGTOs	1·1769	2083·5	2056·3	516
MP4SDQ‡	74 cGTOs	1·1772	2081·7	2054·5	515
MP2	160 cGTOs	1·1843	2004·7	1976·0	546
CCSD	160 cGTOs	1·1709	2140·8	2118·0	467
CCSD(T)	160 cGTOs	1·1785	2074·6	2050·0	495

† [67]; valence electrons correlated.
‡ [68]; all electrons correlated.

was employed in MP2, CCSD and CCSD(T) calculations with all electrons being correlated. Results are shown in table 4. The present CCSD(T) calculations confirm the high quality of the previous predictions. The equilibrium bond length of 1·1785 Å should be accurate to 0·001 Å and the calculated wavenumber of the fundamental vibrational transition of 2050·0 cm^{-1} is expected to have an uncertainty of less than 5 cm^{-1}. This may be compared with the 'free ion' wavenumber of 2038 cm^{-1} as extrapolated by Sherman and Wilkinson [69] from infrared spectra of CN^- isolated in alkali halide lattices. Infrared spectroscopy in a neon matrix [70] yielded 2053 cm^{-1}, very close to the theoretical values. Quite recently, the 266 nm photoelectron (PE) spectrum of CN^- was recorded with a pulsed time-of-flight PE spectrometer [71]. A Franck–Condon analysis yielded $R_e = 1{\cdot}177 \pm 0{\cdot}004$ Å and $\nu_{0-1} = 2035 \pm 40\,cm^{-1}$. Within their error limits both agree with the theoretical values, which are still ahead in accuracy.

3.5. *Electric dipole moments*

As has been shown for CO [72] and HCN [55], CCSD(T) is capable of calculating electric dipole moments to an accuracy of better than 0·01 D. This will probably hold for any small molecule with first-row atoms provided that the Hartree–Fock determinant dominates the total wavefunction and that basis sets almost saturated in the s, p, d, and f parts are employed. The experimental determination of dipole moments of ions is a difficult task since the convenient method for neutrals—measurement of Stark splittings of pure rotational transitions by microwave or millimetre wave spectroscopy—does not work for ions. An alternative method applicable to ions consists in the measurement of the isotopic dependence of the rotational Zeeman effect by means of far-infrared laser spectroscopy as first done for ArH^+ by Laughlin *et al.* [73]. This technique is rather demanding, however, and lacks precision. So far, an accuracy of no better than 0·2 D could be obtained even in favourable cases like HN_2^+ [74]. No experimental dipole moment determination for any molecular anion has yet been carried out. Since the square of the electric dipole moment determines the intensity of pure rotational transitions accurate *ab initio* predictions are of great interest.

Throughout this work electric dipole moments (referring to the molecular centre-of-mass coordinate system) are calculated as energy derivatives and the effects of core and core–valence correlation have been neglected since they turned out to be insignificant in other molecules (see, e.g., [72] and [55]). A comparison of calculated equilibrium and ground-state dipole moments for the diatomic anions OH^-, SH^- and CN^- is made in table 5. The present CCSD(T) values should be accurate to better than 0·01 D.

Downloaded At: 17:15 21 January 2011

Table 5. Equilibrium and ground-state electric dipole moments for OH^-, SH^- and CN^-.

Anion	Method	Basis set	Ref.	μ_e(D)	μ_0(D)
OH^-	CEPA-1	73 cGTOs	[127]	1·054	1·020
	MRCI	73 cGTOs	[127]	1·072	1·039
	CCSD(T)	189 cGTOs	this work	1·068	1·035
SH^-	CEPA-1		[60]	0·273	
	CCSD(T)	193 cGTOs	this work	0·333	0·302
CN^-	CEPA-1	92 cGTOs	[67]	0·639	0·633
	CISD	66 cGTOs	[68]	0·544	
	CCSD(T)	160 cGTOs	this work	0·650	0·645

4. Equilibrium structures of polyatomic anions

Geometric structures of molecules are playing an important role in chemistry. Among the different structures which may be defined, the equilibrium structure appears to be the most satisfactory one (see, e.g., [75]). From the theoretical point of view it corresponds to a global or local minimum of a Born–Oppenheimer potential energy hypersurface and is thus easily amenable to quantum-chemical calculation. On the other hand, the determination of the equilibrium geometry of a polyatomic molecule solely on the basis of experimental data is a notoriously difficult task, even for stable species.

Rather accurate experimental equilibrium structures are so far only available for NH_2^- [15], FHF^- [22] and $ClHCl^-$ [23] through analysis of data from high-resolution infrared laser spectroscopy. Large-scale *ab initio* calculations at the CCSD(T) or a comparable level may yield equilibrium bond lengths of anions with first-row atoms accurate to 0·001–0·002 Å. Results of calculations of this sort are given in table 6.

Still more accurate equilibrium structures may be determined by suitable combination of theoretical and experimental data, provided that the latter are available. Over the past three years we have successfully applied this procedure to a larger number of neutrals and molecular cations (see, e.g., [76] and references therein). Ground-state rotational constants are taken from high-resolution spectroscopic studies while theoretical values are used for the differences between equilibrium and ground-state values. These may be obtained either from variational calculations or by means of conventional second-order perturbation theory in normal coordinate space. For semi-rigid molecules the differences between the two approaches are usually negligibly small and the more economic latter method may be the advantageous one.

Making use of a three-dimensional CEPA-1 potential, the stretching part of which was published earlier [77], the difference $B_e - B_0$ of N_3^- was calculated to be 0·0026 cm^{-1} from variational calculations of rovibrational states [26]. Combining this value with the experimental B_0 value of 0·4262 cm^{-1} [17] one arrives at a NN equilibrium bond length of 1·1850 Å, with an estimated uncertainty of about 0·0005 Å. It compares nicely with the result of the large-scale CCSD(T) calculations of 1·1840 Å given in table 6.

An accurate equilibrium geometry of the amide anion, NH_2^-, was also obtained by combination of experimental and theoretical data. The differences ΔA_0, ΔB_0 and ΔC_0 were calculated from a CCSD(T) anharmonic potential energy hypersurface [78] by conventional perturbation theory according to

$$\Delta A_0 = A_e - A_0 \approx \sum_i \alpha_i^A/2, \tag{1}$$

with the same sort of formulae holding for ΔB_0 and ΔC_0. These were combined with

Downloaded At: 17:15 21 January 2011

Table 6. Equilibrium geometries of triatomic molecular anions type ABC^- from CCSD(T) calculations (all electrons correlated).

Anion	Basis set	R_e^{AB} (Å)	R_e^{BC} (Å)	α_e (°)
NO_2^-	138 cGTOs	1·2578	1·2578	116·56
C_3^- †	255 cGTOs	1·3070	1·3070	180
N_3^-	165 cGTOs	1·1840	1·1840	180
FHF^-	206 cGTOs	1·1380	1·1380	180
		(1·1389)‡	(1·1389)‡	(180)‡
HCC^-	206 cGTOs	1·0683	1·2470	180
NCO^-	138 cGTOs	1·1917	1·2284	180
HO_2^-	115 cGTOs	0·9593	1·5219	97·65

† RCCSD(T) calculations; see section 2.
‡ Experimental values [22].

Table 7. Equilibrium geometries for NH_2^-.

Method	Ref.	r_e (Å)	α_e (°)
CEPA-1†	[87]	1·02998	102·00
MP2	[78]	1·0243	102·58
CCSD	[78]	1·0233	102·32
CEPA-1	[78]	1·0245	102·24
CCSD(T)	[78]	1·0270	102·19
best‡	this work	1·0269(2)	102·15(5)

† Valence electrons correlated.
‡ Mixed experimental/theoretical procedure (see the text).

Downloaded At: 17:15 21 January 2011

the experimental ground-state constants of Tack *et al.* [15] ($A_0 = 691\,042{\cdot}6$ MHz, $B_0 = 391\,735{\cdot}8$ MHz, $C_0 = 243\,464{\cdot}4$ MHz) to yield improved equilibrium rotational constants. The equilibrium geometrical parameters r_e and α_e were then obtained from the three possible combinations of A_e, B_e and C_e and the resulting mean values, with estimated uncertainties quoted in units of the last digit, are $r_e = 1{\cdot}0269(2)$ Å and $\alpha_e = 102{\cdot}15(5)°$. Comparison with results from *ab initio* calculations is made in table 7. Our previous CCSD(T) values [78] are in excellent agreement with the above ones. As is frequently observed, the CEPA-1 results are intermediate between CCSD and CCSD(T) MP2 performs remarkably well but we wish to mention that this method substantially overestimates the stretching vibrational wavenumbers [78].

Some experimental information on the geometric structure of CH_2N^- is available through photoelectron (PE) spectroscopy [79]. However, an exceptionally long CH distance and an unusually small HCH angle were obtained from the simulation of the PE spectrum. Using *ab initio* methods, geometry optimizations have been carried out by Lohr [80] at the SCF/6-31G* and SCF/6-31+G** levels, by Cowles *et al.* [79] within the SCF and MP2 approximations using a 6-31++G** basis set and by Koch and Frenking [81] at the SCF/6-31G* level. We have calculated the equilibrium geometry of CH_2N^- by SCF, MP2, CCSD, CEPA-1 and CCSD(T) using a basis set of 144 cGTOs which is briefly described as follows. The avqz basis set was used for the s and p parts of all atoms. The d functions of carbon and nitrogen were taken from the avtz set and their f functions from the quadrupule-zeta (vqz) set [82]. One set of d functions (from the vtz set) was employed for the hydrogen atoms. All electrons were correlated in the

Downloaded At: 17:15 21 January 2011

Table 8. *Ab initio* equilibrium geometries and total energies for H_2CN^-.

	SCF‡	MP2§	MP4§	CCSD†	CEPA-1†	CCSD(T)†
r_e(CH, Å)	1·1245	1·1385	1·1423	1·1353	1·1373	1·1397
α_e(HCH, °)	109·28	108·32	108·32	108·87	108·88	108·87
R_e(CN, Å)	1·2299	1·2440	1·2525	1·2442	1·2470	1·2502
V_e(+93 E_h)	−0·428797	−0·877845	−0·913110	−0·888670	−0·894163	−0·909919

† This work. All electrons correlated; basis set: 144 cGTOs.
‡ SCF/6-31++G** [79]: r_e = 1·124 Å, α_e = 109° and R_e = 1·240 Å.
§ MP2/6-31++G** [79]: r_e = 1·139 Å, α_e = 108° and R_e = 1·256 Å.

calculations which account for correlation effects. The results are given in table 8. The CCSD(T) equilibrium bond lengths are believed to be accurate to about 0·001 Å, the bond angle to 0·1°. The latter is remarkably small; the corresponding experimental value for isoelectronic formaldehyde [83] is larger by 7·6°. Apparently, the increased size of the essentially non-bonding $2b_2$ orbital in the anion is responsible for this effect. CEPA-1 produces results intermediate between CCSD and CCSD(T) for the equilibrium bond lengths while the bond angle is practically the same for all three methods. The effect of the connected triple substitutions is over-estimated by MP4, which, compared to CCSD(T), yields r_e and R_e too long by 0·0026 and 0·0023 Å, respectively.

The equilibrium geometry of the electronic ground state of C_5^- ($\tilde{X}^2\Pi_u$) has been calculated by RCCSD(T) with a basis set of 170 cGTOs (sp(avtz) + df(vtz)), valence electrons being correlated. The result is: R_{1e} (outer) = 1·2925 Å and R_{2e} (inner) = 1·3066 Å. This equilibrium structure is practically identical to that of Watts and Bartlett [84], which was published in the course of this work. Their PVTZ basis set differs from ours by the omission of the diffuse s function at each carbon atom. Analogous CCSD(T) calculations for C_5 yield R_{1e} = 1·2971 Å and R_{2e} = 1·2885 Å, again in very good agreement with the calculations of Watts and Bartlett. These equilibrium bond lengths are larger than the accurate ones published earlier by one of us [85] by 0·0075 and 0·0066 Å. We expect similar errors in the calculations for C_5^- and therefore recommend a reduction by 0·007 Å, resulting in R_{1e} = 1·2855(15) Å and R_{2e} = 1·2996(15) Å. Estimated error bars in terms of the least significant digit are given in parentheses. The corresponding equilibrium rotational constant is B_e = 2515(6) MHz. It should also provide a good estimate for the ground-state value B_0, since the difference $B_e - B_0$ should be only on the order of 1 MHz.

In an analogous way we predict the equilibrium geometry of C_6^- ($\tilde{X}^2\Pi_u$) to be R_{1e} (outer) = 1·2745(15) Å, R_{2e} (middle) = 1·3248(15) Å and R_{3e} (inner) = 1·2518(15) Å. The corresponding B_e value is 1442 MHz. Compared to the RHF/DZP equilibrium geometry of Watts and Bartlett [86] there are differences of ΔR_{1e} = 0·017 Å, ΔR_{2e} = − 0·015 Å and ΔR_{3e} = 0·015 Å. Assuming the same errors to hold for their RHF/DZP calculations on C_8^- and C_{10}^- we predict the following equilibrium bond lengths for these two species:

(*a*) C_8^- ($\tilde{X}^2\Pi_g$): R_{1e} = 1·274 Å, R_{2e} = 1·322 Å, R_{3e} = 1·249 Å and R_{4e} = 1·317 Å; B_e = 605·4 MHz.

(*b*) C_{10}^- ($\tilde{X}^2\Pi_u$): R_{1e} = 1·273 Å, R_{2e} = 1·321 Å, R_{3e} = 1·248 Å, R_{4e} = 1·316 Å and R_{5e} = 1·246 Å; B_e = 309·5 MHz.

The numbering always starts with the outermost CC bond.

5. (Ro)vibrational term energies

5.1. NH_2^-

Following our earlier work at the CEPA-1 level [87] variationally calculated vibrational term energies have been recently reported for different isotopomers of the amide anion [78]. Four different methods (MP2, CCSD, CEPA-1 and CCSD(T)) and a large basis set of 144 cGTOs were employed in the calculation of the anharmonic potential energy hypersurface. The results of the CCSD(T) calculations turned out to be in excellent agreement with available experimental data from high-resolution infrared spectroscopy [15]. The calculated band origins of the stretching vibrations differed from experiment by only 1·6 cm^{-1} (ν_1) and 5·4 cm^{-1} (ν_3). The wavenumber

Downloaded At: 17:15 21 January 2011

of the bending vibration was predicted to be 1449·5 cm^{-1}, with an uncertainty of less than 5 cm^{-1}. In agreement with previous theoretical work [88] the absolute infrared intensity of this band is calculated to be very small (1·5 km mol^{-1}). This is in severe disagreement with the assignment of matrix absorptions made by Suzer and Andrews [89], which thus appears to be incorrect. As is frequently observed for AH_2 molecules, a slight Fermi resonance was found between the first excited state of the symmetric stretching vibration (ν_1) and the first overtone of the bending vibration ($2\nu_2$). It has the effect that the intensity of the first overtone is larger than that of the bending fundamental.

5.2. NCO^-

Gruebele, Polak and Saykally [19] have measured 132 rovibrational transitions in the ν_3 (pseudoantisymmetric stretch) fundamental and three accompanying hot bands of the cyanate anion (NCO^-) making use of tunable diode laser spectroscopy and employing the velocity modulation technique. Theoretical work on NCO^- is scarce and, regarded from present day's standard, has been carried out at a rather low level [81]. Making use of CCSD(T) and the avtz basis set (138 cGTOs) we have calculated a three-dimensional anharmonic potential energy function (see table 9), subsequently used in calculations of the low-lying rovibrational states. Rovibrational energies of NCO^- are calculated by the DVR-DGB method [90, 91], which makes use of a discrete variable representation (DVR) for the angular variable and a real two-dimensional distributed Gaussian basis (DGB) for the radial degrees of freedom. The vibration–rotation Hamiltonian is formulated in Jacobi coordinates. The rovibrational states were assigned by identifying a leading coefficient of the wavefunction expansions in the adiabatic basis set formulated at the DVR level [92]. Parameters from effective (spectroscopic) Hamiltonians like vibrational term energies T_v, rotational constants B_v, centrifugal distortion D_v and l-type doubling q_v constants are determined and compared with available experimental data in table 10.

The band origin of the bending vibration is predicted to be 621·8 cm^{-1} with an accuracy of about 5 cm^{-1}. As for isoelectronic CO_2, a strong Fermi resonance is found

Table 9. CCSD(T) potential energy function for NCO^-† (all electrons correlated).

PEF term				PEF term			
value‡	i	j	k	value‡	i	j	k
0·480179	2	0	0	−0·053557	1	2	0
−0·577490	3	0	0	0·051466	2	2	0
0·411746	4	0	0	0·027679	1	3	0
−0·252035	5	0	0	0·004684	3	1	0
0·125184	6	0	0	0·083148	0	0	2
0·349923	0	2	0	0·014737	0	0	4
−0·435911	0	3	0	−0·001321	0	0	6
0·329622	0	4	0	−0·063543	0	1	2
−0·201732	0	5	0	−0·013253	0	2	2
0·101970	0	6	0	−0·074679	1	0	2
0·076937	1	1	0	−0·016397	2	0	2
−0·031341	2	1	0	0·035179	1	1	2

† Equilibrium bond lengths: R_{1e} (NC) = 1·1917 Å and R_{2e} (CO) = 1·2284 Å. The expansion $V - V_e = \Sigma_{ijk}\Delta R_1^i \Delta R_2^j \Delta\theta^k$ is employed (k even) where θ measures the deviation from linearity.
‡ In atomic units.

Downloaded At: 17:15 21 January 2011

Downloaded At: 17:15 21 January 2011

Table 10. *Ab initio* CCSD(T) and experimental spectroscopic constants for NCO^- ($l \leqslant 2; T_v \leqslant 3500\,cm^{-1}$).

			$T_v(cm^{-1})$†		$B_v(cm^{-1})$		$q_v(10^{-4}cm^{-1})$		$D_v(10^{-7}cm^{-1})$	
v_1	v_2^l	v_3	calc.	exp.†	calc.	exp.	calc.	exp.	calc.	exp.
0	0^0	0	0	0	0·38317	0·384144(44)			1·49	1·54(11)
0	1^1	0	621·785	(623·3)	0·38379	0·384862(28)	6·56	6·58(28)	1·52	1·908(10)
1	0^0	0	1187·193	(1195·7)	0·38282	0·382112(94)			1·74	1·35(56)
0	2^2	0	1244·713		0·38441	0·385403(78)‡			1·57	
0	2^0	0	1275·600	(1282·6)	0·38331				1·24	1·91(54)
1	1^1	0	1791·757	(1801·2)	0·38356		9·34		1·73	
0	3^1	0	1914·205	(1922·7)	0·38379		10·59		1·36	
0	0^0	1	2137·475	2124·308(1)	0·38021	0·381163(42)			1·49	1·54(10)
2	0^0	0	2358·467	(2374)	0·38295				2·05	
1	2^2	0	2401·471		0·38423				1·68	
1	2^0	0	2451·975	(2469·9)	0·38222				1·35	
0	4^2	0	2549·820		0·38432				1·57	
0	4^0	0	2571·157	(2581)	0·38366				0·97	
0	1^1	1	2747·842	(2756·5)	0·38086	0·381908(28)	6·35	6·37(28)	1·51	1·885(10)
2	1^1	0	2949·243		0·38357		12·78		1·97	
1	3^1	0	3076·149		0·38307		12·29		1·48	
0	5^1	0	3219·908		0·38394		15·43		1·21	
1	0^0	1	3304·441	(3319·6)	0·38993	0·379123(104)			1·74	1·35§
0	2^2	1	3359·390		0·38150	0·382495(80)‡			1·54	
0	2^0	1	3390·878	(3406·0)	0·38036				1·22	1·91§

† Values in parentheses refer to NCO^- isolated in CsI [128].
‡ Reassignment made; see the text.
§ Assumed.

between the pseudosymmetric stretching vibration v_1 and the first overtone of the bending vibration v_2^l with vibrational angular momentum quantum number $l = 0$. The corresponding vibrational wavefunction expansions in the adiabatic basis $|v_1\, v_2^l\, v_3|$ have the following leading terms:

$$\Psi_{\mathrm{I}} = 0{\cdot}787|0\,2^0\,0\rangle - 0{\cdot}615|1\,0^0\,0\rangle + \ldots,$$

$$\Psi_{\mathrm{II}} = -0{\cdot}614|0\,2^0\,0\rangle - 0{\cdot}788|1\,0^0\,0\rangle + \ldots,$$

where the roman numbers I and II denote the upper and lower components, respectively, of the Fermi diad. The corresponding band origins are calculated to be 1275·6 and 1187·2 cm^{-1}. Both components of the Fermi diad exhibit almost equal expectation geometries as a consequence of the very strong mixing of the zero-order functions in Ψ_{I} and Ψ_{II}. The expectation values $\langle R_1(\mathrm{NC})\rangle$ and $\langle R_2(\mathrm{CO})\rangle$ are 1·199 and 1·238 Å, respectively, for both Ψ_{I} and Ψ_{II}; the expectation values for the deviation from linearity are $\langle\alpha_{\mathrm{I}}\rangle \approx 10°$ and $\langle\alpha_{\mathrm{II}}\rangle \approx 11°$ for Ψ_{I} and Ψ_{II}, respectively. The present value for the band origin of the pseudoantisymmetric stretching vibration v_3 of 2137·5 cm^{-1} is overestimated by 13·2 cm^{-1} or 0·6% when compared to the corresponding experimental value of 2124·3 cm^{-1} [19].

The ground-state rotational constant $B_{(0\,0^0\,0)}$ is calculated to be 0·38317 cm^{-1}, i.e. 0·25% below the experimental value [19]. This is an indication that the calculated equilibrium bond lengths, $R_{1e} = 1{\cdot}1918$ Å and $R_{2e} = 1{\cdot}2284$ Å, are too long by 0·001–0·002 Å, probably mainly due to neglect of g functions in the basis set. The calculated difference in the rotational constant $\Delta B_3 = B_{(0\,0^0\,0)} - B_{(0\,0^0\,1)}$ of 0·00296 cm^{-1} is in excellent agreement with the experimental value of 0·0029806(22) cm^{-1}. Our calculations suggest a misassignment in the work of Gruebele *et al.* [19]. The hot band with origin at 2101·228(4) cm^{-1} should have the initial state $(0\,2^2\,0)$ and the final state

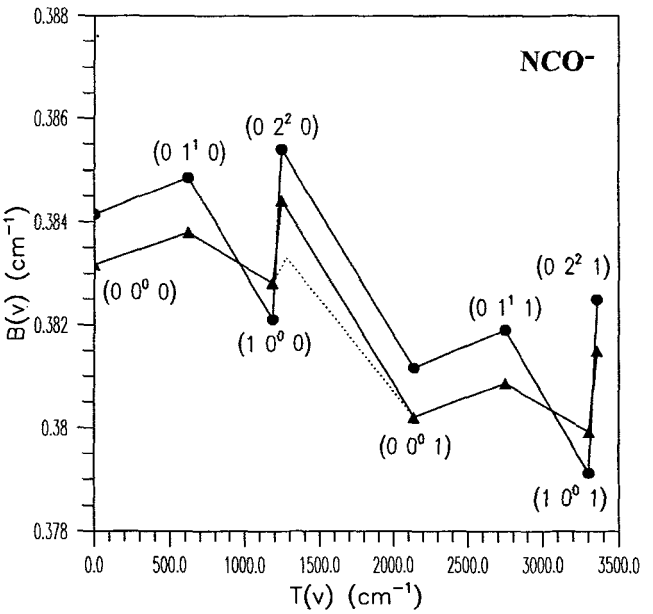

Figure 2 Comparison of rotational constants B calculated in this work (solid triangles) with available experimental values (solid circles) for NCO^-. The position of the value $B^{\mathrm{calc}}_{(02^00)}$ is shown by a dotted line.

Downloaded At: 17:15 21 January 2011

$(0\,2^2\,1)$ instead of the $l = 0$ components. The strong Fermi resonance produces almost identical rotational constants for the two components of each Fermi diad, which is at variance with the analysis of [19]. Transitions arising from the $(0\,2^0\,0)$ level (upper component of the Fermi diad) may well be hidden under the stronger fundamental band since we calculate an almost identical rotational constant for this state compared with the vibrational ground state.

A graphical comparison of the theoretical B^{calc} and experimental B^{exp} rotational constants is made in figure 2. It is evident that after the reassignment B^{calc} and B^{exp} reveal the same behaviour. All rotational constants listed in table 10 agree with the corresponding experimental values to better than 0·28%. The almost perfect agreement between q^{exp} and q^{calc} for the levels $(0\,1^1\,0)$ and $(0\,1^1\,1)$ levels should also be emphasized.

5.3. NO_2^-

No high-resolution experimental investigation is yet available for NO_2^- which is regarded as an end product in the upper atmosphere's negative ion chemistry [93]. Vibrational frequencies have been determined by low-resolution photoelectron spectroscopy (PES) [94] and matrix infrared spectroscopy [95–97]. The potential energy surface of NO_2^- was calculated by CCSD(T) with the avtz basis (all electrons correlated). It is analytically represented by the expression

$$V - V_e = \sum_{ijk} C_{ijk} \Delta R_1^i \Delta R_2^j \Delta\alpha^k. \tag{2}$$

The internal coordinates ΔR_1, ΔR_2 and $\Delta\alpha$ are differences of the bond lengths and the bond angle with respect to the equilibrium values (see table 6). The coefficients C_{ijk} are listed in table 11. Therefrom vibrational term energies were calculated variationally; the results are given in table 12. Like the previous CASSCF and corrected values of Peterson *et al.* [98] the present CCSD(T) values lie well within the error bars of the data

Table 11. CCSD(T) potential energy function for NO_2^- † (all electrons correlated).

PEF term				PEF term			
value‡	i	j	k	value‡	i	j	k
0·252229	2	0	0	0·123240	1	1	0
−0·345460	3	0	0	−0·069658	2	1	0
0·289098	4	0	0	−0·043428	2	2	0
−0·182271	5	0	0	0·037115	3	1	0
0·093662	6	0	0	0·073476	1	0	1
−0·021310	7	0	0	−0·196519	1	0	2
−0·008760	8	0	0	−0·080358	2	0	1
0·280741	0	0	2	0·017559	2	0	2
−0·154418	0	0	3	0·155940	1	0	3
0·115445	0	0	4	0·011554	3	0	1
−0·089721	0	0	5	−0·153157	1	1	1
0·046379	0	0	6	0·134617	2	1	1
−0·020287	0	0	7	0·212230	1	1	2
−0·003453	0	0	8				

† Only non-redundant terms are quoted. Geometrical parameters see table 6.
‡ In atomic units.

Downloaded At: 17:15 21 January 2011

Table 12. Vibrational term energies of NO_2^- (in cm^{-1}).

Band	theor.†[98]	exp. [94, 97]	this work
ν_2	782	776 ± 30	781·8
ν_3	1232	1241·5‡	1258·1
ν_1	1286	1284 ± 30	1288·2
$2\nu_2$	1563		1562·4
$\nu_2 + \nu_3$			2027·4
$\nu_1 + \nu_2$			2063·1
$3\nu_2$			2341·8
$2\nu_3$			2493·2
$\nu_1 + \nu_3$		2509·6	2524·7
$2\nu_1$			2570·2

† Results from empirically corrected *ab initio* calculation.
‡ Neon matrix value.

obtained by PES. The present ν_3 band origin should be accurate to about $10\,cm^{-1}$; thus the corrected value of Peterson *et al.* [98] is probably still an underestimate. A matrix shift to the red by $18\,cm^{-1}$ is not unusual for a negative ion.

5.4. HO_2^- and DO_2^-

Making use of variational calculations with a three-dimensional CCSD(T) potential (basis: avtz; 115 cGTOs), the band origins of the fundamentals of HO_2^- and DO_2^- (in parentheses) are predicted to be 3585 (2657), 1074 (821), and 729 (711) cm^{-1}. These values are believed to be accurate to about $10\,cm^{-1}$. The corresponding harmonic vibrational frequencies are calculated to be 3810 (2776), 1120 (843) and 758 (740) cm^{-1}. Very crude experimental ν_3 values of $775 \pm 250\,cm^{-1}$ (HO_2^-) and $900 \pm 250\,cm^{-1}$ (DO_2^-) are available through photoelectron spectroscopy [99]. These authors also calculated *ab initio* harmonic vibrational frequencies. They made use of the perfect-pairing generalized valence bond (GVB/PP) method augmented by two types of limited configuration interaction (CI) denoted GVB-CI and POL-CI. Employing a modestly large basis set of 'DZP + diffuse' quality the most extensive POL-CI calculations yielded $\omega_1 = 3662\,cm^{-1}$, $\omega_2 = 1153\,cm^{-1}$, $\omega_3 = 821\,cm^{-1}$. More recently, the anharmonic frequencies of HO_2^- were calculated by means of a simple one-dimensional approach (per internal coordinate) making use of the results of MRD-CI calculations with a moderately large basis set of 52 cGTOs [100]. Values of 3650, 1170 and $833\,cm^{-1}$ were obtained for HO_2^-. We have checked the performance of this approach against our accurate procedure (for the given potential) and found that it produces a rather large error of 9% ($66\,cm^{-1}$) for the OO stretching vibration ν_3.

5.5. HCC^-: *An Eyring's lake on top of the barrier to H migration*

The acetylide anion HCC^- is one of the simplest carbanions. In the ground electronic ($\tilde{X}^1\Sigma^+$) state it has a linear equilibrium geometry (see section 4 for accurate equilibrium bond lengths). The first gas-phase spectrum unambiguously assigned to HCC^- was reported by Ervin and Lineberger [27] who made use of photodetachment techniques. The observed fundamental wave-numbers of HCC^- are $505 \pm 20\,cm^{-1}$ for the ν_2 bending vibration and $1800 \pm 20\,cm^{-1}$ for the ν_3 CC stretching vibration. The stability of the HCC^- anion accounts for the high electron affinity [27] of $2{\cdot}969 \pm 0{\cdot}006$ eV for the C_2H radical.

Downloaded At: 17:15 21 January 2011

Table 13. CEPA-1 and experimental vibrational term energies for different isotopomers of the acetylide anion†.

v_1	v_2	v_3	$T_{exp}^{HCC^-}$	$T_{calc}^{HCC^-}$	v_1	v_2	v_3	$T_{exp}^{D^{13}C_2^-}$	$T_{calc}^{D^{13}C_2^-}$
0	0	0	0·0	0·0	0	0	0	0·0	0·0
0	1	0	505	512·488	0	1	0	385	402·055
0	2	0	1015	1007·075	0	2	0	795	792·849
0	0	1	1800	1814·867	0	0	1	1655	1669·755
0	1	1	2300	2320·519	0	1	1		2070·176
1	0	0		3216·724	1	0	0		2447·035
1	1	0		3709·619	1	1	0		2834·315
1	0	1		5018·745	1	0	1		4094·881
1	1	1		5505·982	1	1	1		4480·282
	?		[3435]			?		[3310]	
0	3	1		3216·724	0	4	1		3239·132
0	7	0		3436·706	0	0	2		3325·100
0	0	2		3611·286	0	9	0		3456·131

† Experimental data from [27]; uncertainty $\pm 20\,cm^{-1}$ except for values in brackets, which have an uncertainty of $\pm 40\,cm^{-1}$.

Downloaded At: 17:15 21 January 2011

A three-dimensional analytical potential has been developed by Sebald [101] on the basis of CEPA-1 calculations with a basis set of 98 cGTOs.

The interesting feature of the calculated potential energy surface is a shallow T-shaped local energy minimum lying 7587 cm^{-1} above the energy at linear geometries [102]. Two equivalent saddle points are lying 271 cm^{-1} above the T-shaped well. Rather similar results were obtained from much more extended CCSD(T) calculations.

Vibrational term energies calculated for HCC^- and $D^{13}C^{13}C^-$ by the DVR-DGB method [90, 91] are compared with corresponding experimental data [27] in table 13. The calculated values agree with the experimental ones within the uncertainty of the latter. In table 13 transitions non-assigned in photoelectron spectra [27] are marked with '?'. Three calculated transitions in their vicinity are listed below. On the basis of our calculations it is questionable that the peaks belong to the noted isotopic species.

The energy levels up $\sim 13\,600\,cm^{-1}$ relative to the minima at linear geometry were investigated in particular detail. In the energy interval studied here there are 169 vibrational ($J = 0$) levels most of which, i.e. 136, can be readily assigned. The fraction of the states associated with a dominant coefficient squared smaller than 0·5, whose assignment was thus uncertain, is very small, i.e. five out of 169 levels. Consequently, a largely regular spectral behaviour is to be expected for the energies considered. The tunnelling splitting calculated is rather small, for instance the splitting in the $(0\,14^0\,0)$ pair is found to be $1{\cdot}69\,cm^{-1}$.

Figure 3 shows three sets of pairs of eigenstates which exhibit the strong mixing between zero-order components. The nodal pattern of the wavefunctions in the region of the T-shaped well differs prominently from the pattern in the remaining molecular space in particular for the $n^{0,0} = 117,121$ pair. Here $n^{J,p}$ stands for the ordinal number for J and parity p. When the potential energy surface was modified by suppressing the T-shaped well (setting V simply constant over the region $75° \leqslant \theta \leqslant 105°$), the two pairs $n^{0,0} = 104, 105$ and $n^{(0,0)} = 167, 168$ displayed weaker mixing and their assignment was possible to make. Detailed analysis has shown that the levels $n^{0,0} = 104, 105, 117, 121, 167$, and 168 (see figure 3) have the origin in the $(0\,16^-\,1)$, $(0\,22^-\,0)$, $(0\,24^+\,0)$,

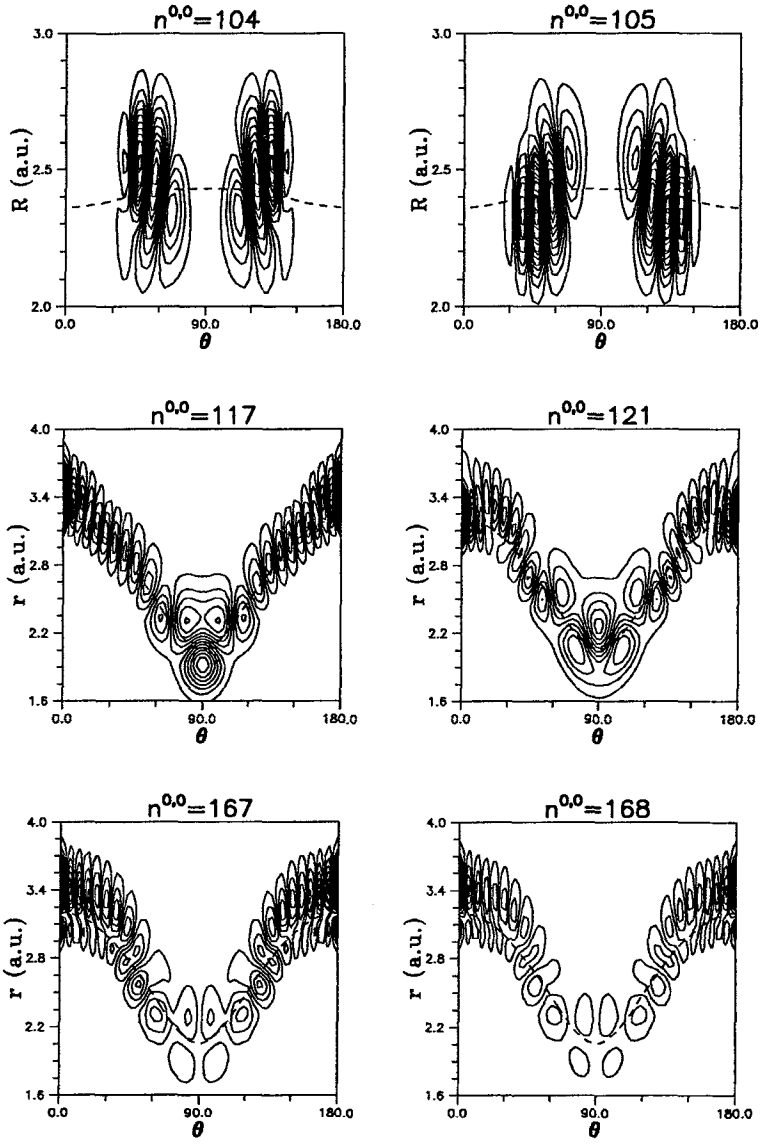

Figure 3. Wavefunctions for vibrational states which exhibit strong mixing of zero-order components in Jacobi (θ, R, r) space with the third coordinate fixed at its expectation value. Here, R is the CC bond length, and r is the distance between the H atom and the centre of mass of the CC unit.

$(1\,14^{+}\,0)$, $(0\,16^{-}\,2)$, and $(0\,22^{-}\,1)$ zero-order components, respectively, where the double-well symmetry is indicated by + or − superscripts. The two states in each pair exhibit very similar expectation geometries.

The anharmonicity of the bending vibration and the (v_1, v_2) coupling display an important influence on the internal dynamics of HCC^-. In addition, rotation tends to couple the v_1 and v_2 vibrational modes and produces a complex rovibrational structure with Coriolis-type resonances strongly present. The rovibrational levels with the origin in $v_2 > 16$ exhibit particularly strong $(k, k \pm 1)$ Coriolis mixing in the energy region

Downloaded At: 17:15 21 January 2011

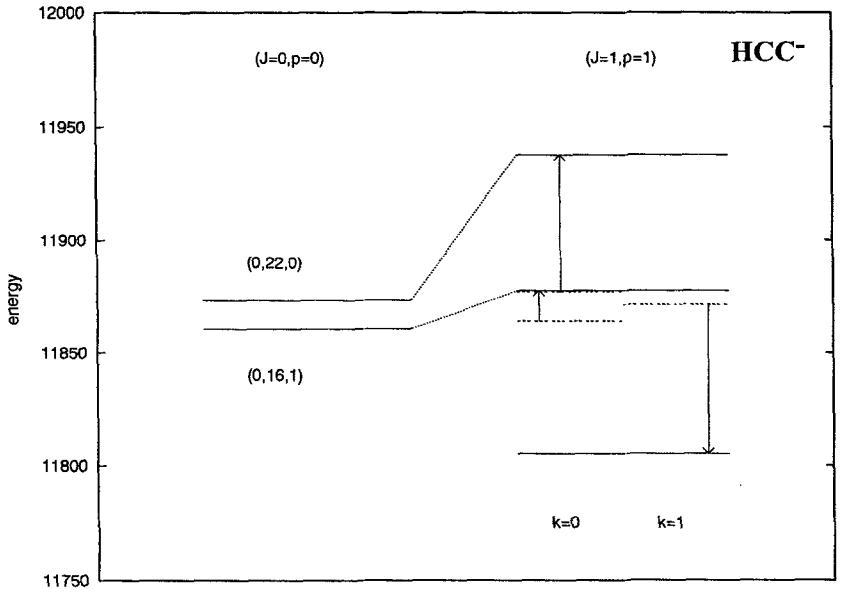

Figure 4. Schematic representation of rotational excitation of the $n^{0,0} = 104, 105$ pair. Exact eigenstates $E^{J,p}$ (solid line) and k-block eigenvalues ${}^{(J)}E^{k}$ (dashed line) are shown for $J = 0$ and $J = 1$ in higher parity. The ${}^{(J)}E^{k}$ levels are connected by an arrow with the exact eigenstates $E^{J,p}$ which have the origin in them. Here, quantum numbers k and l are equal for linear molecules.

considered. The region where the Coriolis resonances are prominent is strongly related to the onset of the free-rotor limit.

Additionally, the Coriolis-type interaction can affect the mixing of the zero-order components (see figure 4). Here rotational excitation of the $n^{0,0} = 104, 105$ pair is schematically shown for $J = 1$. Once rotation is excited the level with the origin in $(0\,22^{-}\,0)$ and $k = 0$ is largely involved in the Coriolis resonance with the $(0\,23^{+}\,0)$ and $k = 1$ level. The corresponding k-block eigenvalues are pressed apart by $\pm 60\,\mathrm{cm}^{-1}$.

6. Absolute infrared intensities

Almost no experimental information exists for the absolute infrared intensities and the corresponding radiative lifetimes of polyatomic anions. Reliable predictions from *ab initio* calculations including electron correlation and vibrational anharmonicity effects have so far been made for N_3^- [103], $HLiH^-$ [104], $ClHCl^-$ [105], $Cl^- \cdots HF$ [101, 102] and NH_2^- [78]. Here we will concentrate on the absolute infrared intensities for the stretching vibrations of HCC^- and HC_4^- and compare them with the results of calculations for the corresponding isoelectronic neutrals HCN and HC_3N.

While the CH stretching vibration (ν_1) of HCN is more intense than the very weak CN stretching vibration (ν_3) by about three orders of magnitude the situation is opposite for HCC^-. This has been found in earlier work by Botschwina [26, 106] and Lee and Schaefer [107]. The former calculations which were carried out at the CEPA-1 level, yielded $A(\nu_1) = 6{\cdot}0$ and $A(\nu_3) = 62{\cdot}5\,\mathrm{km\,mol}^{-1}$. In that work as well as in the present one the infrared intensities of stretching vibrational transitions between the vibrational ground state $|\Psi_0\rangle$ and the final state $|\Psi_f\rangle$ are calculated according to the formula

$$A_{f0} = \frac{\pi N_A}{3\hbar c \epsilon_0} \tilde{\nu}_{f0} |\langle \Psi_f | \boldsymbol{\mu} | \Psi_0 \rangle|^2. \tag{3}$$

Downloaded At: 17:15 21 January 2011

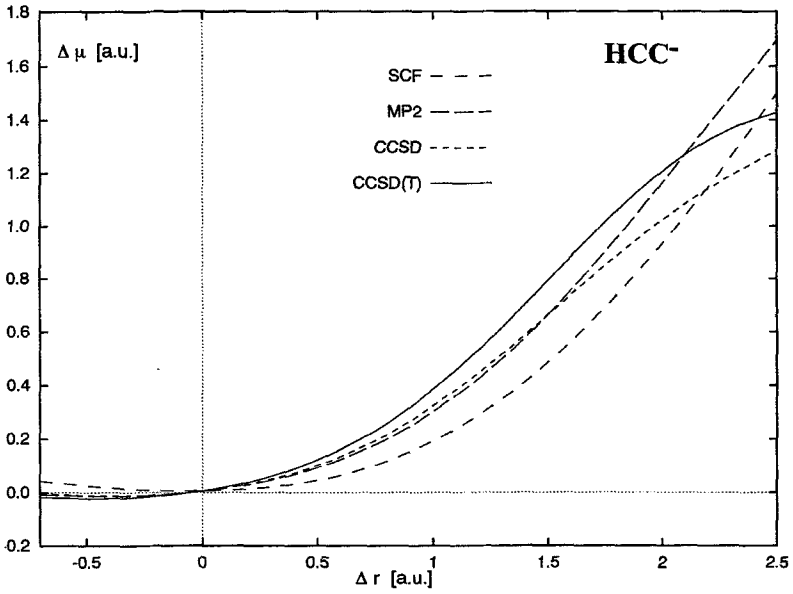

Figure 5. Dependence of the electric dipole moment of HCC^- on the CH stretching vibrational coordinate.

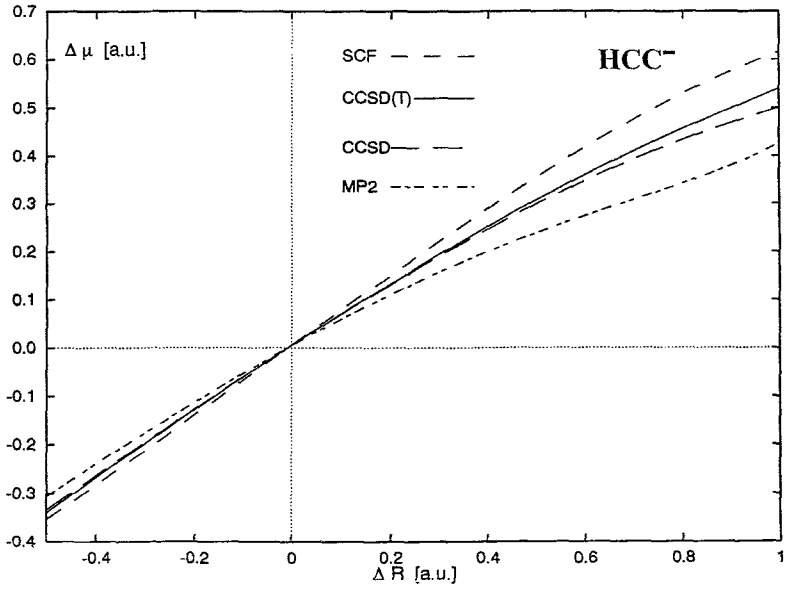

Figure 6. Dependence of the electric dipole moment of HCC^- on the CC stretching vibrational coordinate.

Downloaded At: 17:15 21 January 2011

Table 14. Wavenumbers (in cm^{-1}) and absolute infrared intensities (in $km\,mol^{-1}$) for stretching vibrational transitions of HCC^- and HCN†.

	HCC^-		HCN
Band	$\bar{\nu}$	A	A
ν_3	1792·2	72·36	0·119
ν_1	3196·0	5·239	61·24
$2\nu_3$	3565·3	0·314	0·2(−3)
$\nu_1+\nu_3$	4975·3	0·337	0·290
$3\nu_3$	5319·7	0·017	0·2(−3)
$2\nu_1$	6271·1	1·148	1·263
$2\nu_1+\nu_3$	8036·9	7·9(−3)	0·013
$3\nu_1$	9225·4	0·038	0·030
$3\nu_1+\nu_3$	10975·8	1·2(−3)	1·2(−3)
$4\nu_1$	12059·2	1·9(−3)	1·8(−3)‡

† CCSD(T)/137 cGTO.
‡ Including intensity of near-by band $2\nu_1+3\nu_3$.

Downloaded At: 17:15 21 January 2011

Here, the fundamental constants have their usual meaning and $\bar{\nu}_{f0}$ is the wavenumber of the transition. The quantity A_{f0} is conveniently given in $km\,mol^{-1}$. Alternatively, one may quote the integrated molar absorption cross-section Γ_{f0} (usual unit: $cm^2\,mol^{-1}$), which is approximately related to A_{f0} by

$$\Gamma_{f0} \approx \frac{A_{f0}}{\bar{\nu}_{f0}}. \tag{4}$$

In this work, the variation of the electric dipole moment with the stretching coordinates Δr (CH stretch) and ΔR (CC stretch) has been calculated by various methods using a basis set of 137 cGTOs and correlating the valence electrons. Plots of the diagonal parts of the electric dipole moment functions are given in figures 5 and 6. Most credit should be given to the CCSD(T) results.

The slope of the curve $\Delta\mu(\Delta r)$ at equilibrium is quite small; the CCSD(T) curve is rather strongly nonlinear and develops a maximum around $\Delta r = 2{\cdot}5\,a_0$. On the other hand, the $\Delta\mu(\Delta R)$ curve is much steeper and deviates not very strongly from linearity over the range $-0{\cdot}5\,a_0 \leqslant \Delta R \leqslant 1{\cdot}0\,a_0$. The present results are in good agreement with the earlier CEPA-1 values. While the fundamentals of HCC^- and HCN have very different intensities, the intensities of the overtones of the CH stretching vibrations are very similar. Wavenumbers and absolute infrared intensities of stretching vibrations, calculated variationally from an approximate vibrational Hamiltonian [99, 100], are compared with the corresponding data for HCN [101] in table 14. The present results are in good agreement with the earlier CEPA-1 values.

HC_4^- has a linear equilibrium geometry with $r_e = 1{\cdot}0633$ Å, $R_{1e} = 1{\cdot}2294$ Å, $R_{2e} = 1{\cdot}3743$ Å and $R_{3e} = 1{\cdot}2610$ Å (CCSD(T)/169 cGTO). The equilibrium dipole moment, evaluated in the centre-of-mass coordinate system, is $-6{\cdot}407$ D, with the negative end at the terminal carbon atom. The variation of the electric dipole moment with the stretching vibrational coordinates is shown in figure 7. All three curves involving CC stretching have rather large slopes at equilibrium; on the other hand,

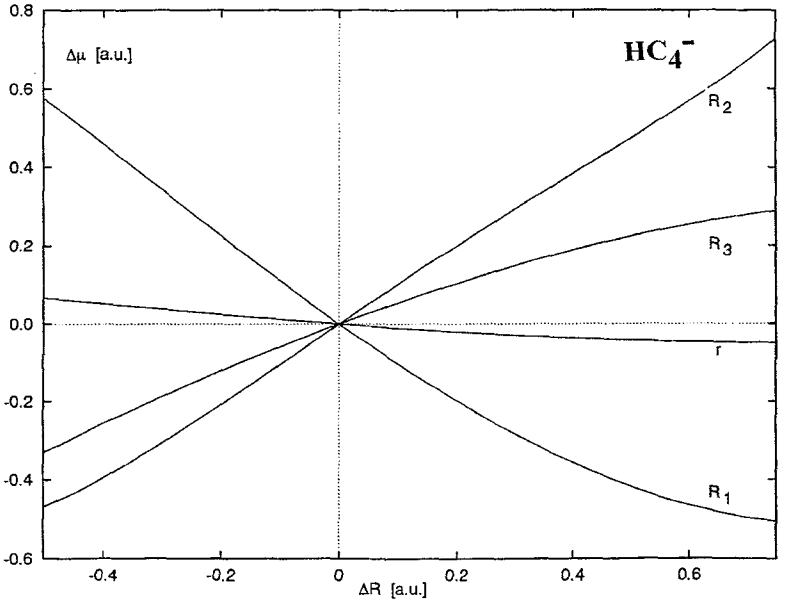

Figure 7. Dependence of the electric dipole moment of HC_4^- on the stretching vibration coordinates (CCSD(T) results).

Table 15. Wavenumbers (in cm^{-1}) and absolute infrared intensities (in $km\,mol^{-1}$) for stretching vibrations of HC_4^-.

Band	$\bar{\nu}$	A	Band	$\bar{\nu}$	A
ν_4	868	13·25	$\nu_1+2\nu_4$	5070	1·5(−3)
$2\nu_4$	1730	1·667	$\nu_1+\nu_3$	5235	0·150
ν_3	1894	2·801	$\nu_1+\nu_2$	5434	0·015
ν_2	2093	609·3	$2\nu_3+2\nu_4$	5495	1·9(−3)
$3\nu_4$	2586	0·196	$3\nu_3$	5644	6·9(−3)
$\nu_3+\nu_4$	2759	0·273	$\nu_2+2\nu_3$	5839	8·5(−3)
$\nu_2+\nu_4$	2958	10·32	$\nu_1+\nu_3+\nu_4$	6098	1·9(−3)
ν_1	3344	65·62	$3\nu_2$	6239	1·1(−3)
$4\nu_4$	3437	0·012	$\nu_1+\nu_2+\nu_4$	6298	4·3(−3)
$\nu_3+2\nu_4$	3618	0·010	$2\nu_1$	6578	1·996
$2\nu_3$	3776	3·732	$\nu_1+\nu_2+\nu_3$	7310	1·7(−3)
$\nu_2+2\nu_4$	3818	0·125	$2\nu_1+\nu_4$	7441	9·6(−3)
$\nu_2+\nu_3$	3972	0·208	$\nu_1+2\nu_2$	7512	1·6(−3)
$2\nu_2$	4172	0·031	$2\nu_1+\nu_3$	8467	6·2(−3)
$\nu_1+\nu_4$	4210	0·192	$2\nu_1+\nu_2$	8666	3·4(−3)
$2\nu_3+\nu_4$	4638	0·064	$3\nu_1$	9704	0·065
$2\nu_2+\nu_4$	5035	2·7(−3)	$4\nu_1$	12727	3·6(−3)

variation of the CH internuclear separation leads only to a small change of the dipole moment.

Wavenumbers and absolute infrared intensities of stretching vibrations are listed in table 15. A very large intensity of $609\,km\,mol^{-1}$ is obtained for the ν_2 band with calculated origin at $2093\,cm^{-1}$. This may easily be rationalized within the familiar double harmonic (DH) approximation which yields $A(\nu_2) = 637\,km\,mol^{-1}$. The

Downloaded At: 17:15 21 January 2011

corresponding normal vibration is rather strongly delocalized and has significant contributions from all three CC stretching coordinates; it may roughly be classified as a pseudo-symmetric CC stretching vibration. This means that the two outer CC bonds expand when the central CC bond contracts and vice versa. The signs of the first dipole moment derivatives at equilibrium are such that all CC stretching contributions appear with equal sign in the evaluation of the normal coordinate derivative $(\frac{\partial \mu}{\partial Q_2})_e$, the square of which is—within the DH approximation—proportional to the absolute infrared intensity.

The second strongest stretching vibration is the ν_1 band ($\sim$ CH stretch) which is weaker than the ν_2 band by one order of magnitude. The other two stretching fundamentals are still weaker, with absolute intensities of only 4·3 and 12·9 km mol^{-1} for ν_3 and ν_4, respectively.

The situation in HC_4^- differs strongly from that in isoelectric HC_3N. Here, the first derivatives of the dipole moment with respect to the heavy-atom stretching vibrational coordinates, taken at equilibrium, have opposite sign compared to HC_4^- and are considerably smaller in magnitude. According to comparable CCSD(T) calculations [110], small intensities of 11·8, 2·65 and 0·17 km mol^{-1} are obtained for the ν_2, ν_3 and ν_4 bands. The ν_1 band is the strongest with $A(\nu_1) = 63{\cdot}5$ km mol^{-1}. All values are in good agreement with experiment [111, 112].

Wavenumbers and absolute infrared intensities of the bending vibrations of HC_4^- were calculated within the DH approximation. The results ($\omega_5 - \omega_7$) are 591, 412 and 206 cm^{-1} and 84·3, 41·9 and 0·59 km mol^{-1}.

Downloaded At: 17:15 21 January 2011

7. Photoelectron spectra and electron affinities

7.1. *The photoelectron spectra of SiH_3^- and SiD_3^-*

The photoelectron (PE) spectra of SiH_3^- and SiD_3^- have been measured by Nimlos and Ellison [113] and adiabatic electron affinities of $1{\cdot}406 \pm 0{\cdot}014$ eV and $1{\cdot}386 \pm 0{\cdot}022$ eV were derived for the two isotropic species. SiH_3^- is strongly pyramidal with a large barrier height to inversion, while SiH_3 has a much lower barrier height and a significantly smaller angle to planarity. One may thus expect significant vibrational structure in the PE spectrum as is indeed observed.

The vibrational structure of the first band of the PE structure of SiH_3^- has been calculated within a two-dimensional anharmonic model which was previously applied to CH_3 [109], H_3O^+ [115], NH_3 [25, 26, 106] and CCl_3 [116] and which takes the symmetric stretching and umbrella bending vibrations into account (for details see [115]).

Two-dimensional CEPA-1 potential energy surfaces for SiH_3^- and SiH_3 are shown in the form of contour plots in figure 8. Therefrom, vibrational term energies, vibrational wavefunctions and Franck–Condon factors have been calculated. The latter are assumed to be proportional to the relative intensities of the peaks observed in a PE spectrum.

A low-temperature stick spectrum for SiH_3^- is shown in figure 9; it takes only transitions from the $(v_1, v_2) = (0, 0^{\pm})$ levels of the anion into account. As is obvious from figure 9 the spectrum is relatively complex and contains a number of near-by peaks. The corresponding term energies of the radical are listed in table 16.

The calculated photoelectron spectrum of SiH_3^- is shown in figure 10. Best agreement with experiment was obtained for a vibrational temperature of 450 K. Peaks A (hot band) and F are those which react most sensitively on the temperature. Agreement with the high signal-to-noise (S/N) PE spectrum of Nimlos and Ellison

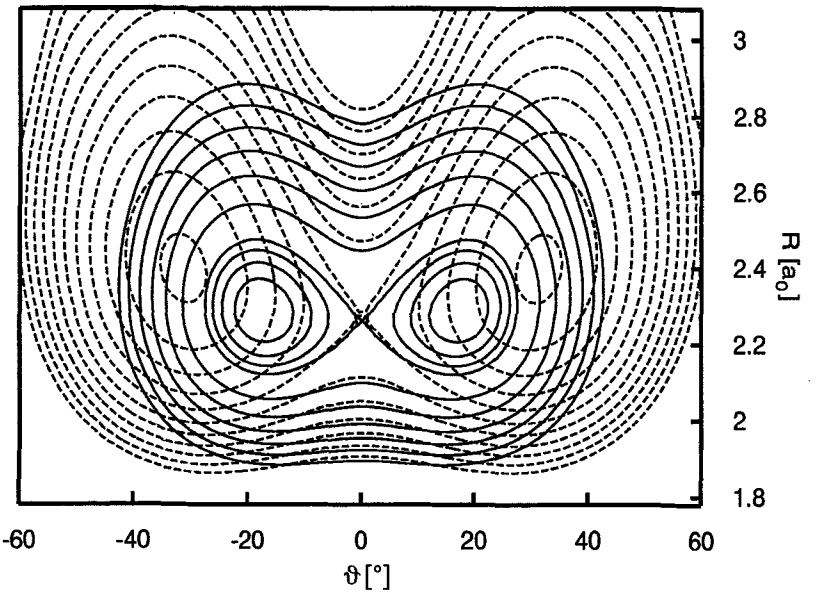

Figure 8. Two-dimensional potential energy surfaces for SiH_3 (solid lines) and SiH_3^- (dashed lines). Contour lines are given in intervals of 2000 cm^{-1} with the exception of the lines below the barrier height of SiH_3, where intervals of 500 cm^{-1} are employed.

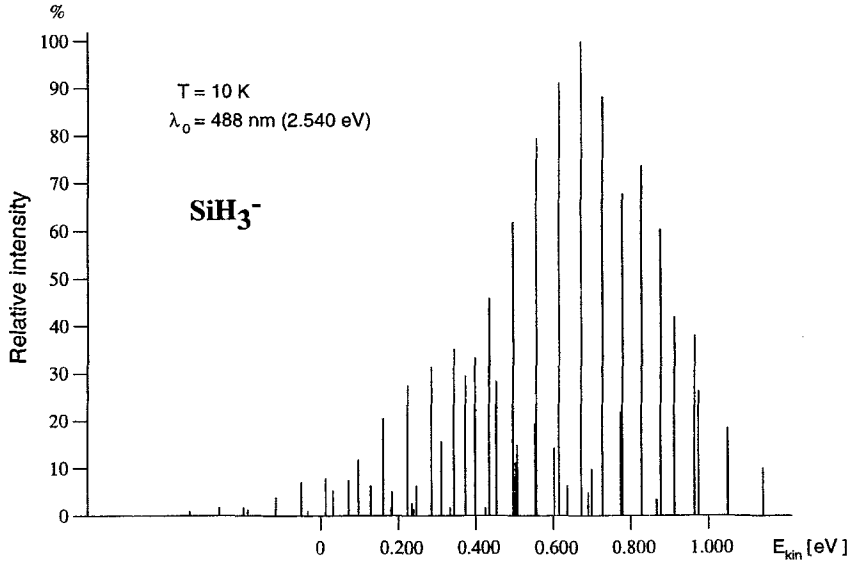

Figure 9. Low-temperature photoelectron stick spectrum of SiH_3^-.

Downloaded At: 17:15 21 January 2011

Table 16. Vibrational term energies for SiH_3 and SiD_3 and Franck–Condon factors for the transition arising from the $(0,0^{\pm})$ state of SiH_3^- and SiD_3^- †.

SiH_3				SiD_3			
v_1	v_2	$\bar{\nu}$	FC factor	v_1	v_2	$\bar{\nu}$	FC factor
0	0^+	0·0	0·0080	0	0^+	0·0	0·0015
0	0^-	0·2	0·0080	0	0^-	0·0	0·0015
0	1^+	724·1	0·0282	0	1^+	547·6	0·0077
0	1^-	730·6	0·0293	0	1^-	547·9	0·0077
0	2^+	1336·8	0·0423	0	2^+	1060·3	0·0187
0	2^-	1421·5	0·0596	0	2^-	1066·2	0·0196
0	3^+	1844·1	0·0660	0	3^+	1495·0	0·0256
0	3^-	2127·9	0·0977	0	3^-	1556·9	0·0323
1	0^+	2210·3	0·0019	1	0^-	1575·7	0·0046
1	0^-	2210·8	0·0044	0	4^+	1859·1	0·0396
0	4^+	2518·8	0·1185	0	4^-	2057·0	0·0564
0	4^-	2908·7	0·1111	1	1^+	2124·0	0·0028
1	1^+	2938·2	0·0073	1	1^-	2125·1	0·0069
1	1^-	2946·5	0·0362	0	5^+	2332·0	0·0727
0	5^+	3335·9	0·1466	0	5^-	2602·1	0·0707
1	2^+	3563·4	0·0155	1	2^+	2639·5	0·0074
1	2^-	3634·8	0·0079	1	2^-	2647·5	0·0264
0	5^-	3777·7	0·1585	0	6^+	2899·3	0·0982
1	3^+	4068·9	0·0102	1	3^+	3081·6	0·0143
0	6^+	4235·4	0·1482	1	3^-	3130·0	0·0016
1	3^-	4337·6	0·0231	2	0^-	3141·9	0·0018
0	6^-	4705·9	0·1256	0	6^-	3207·1	0·1208
1	4^+	4728·9	0·0317	1	4^+	3443·2	0·0048
1	4^-	5106·8	0·0244	0	7^+	3523·4	0·1231
2	1^-	5138·0	0·0182	1	4^-	3633·6	0·0182
0	7^+	5189·7	0·0997	2	1^-	3690·1	0·0027
1	5^+	5537·9	0·0474	0	7^-	3847·4	0·1127
0	7^-	5683·9	0·0724	1	5^+	3910·7	0·0028
2	2^+	5763·5	0·0028	1	5^-	4174·2	0·0270
1	5^-	5979·2	0·0547	0	8^+	4181·9	0·1013
0	8^+	6187·3	0·0469	2	2^-	4217·5	0·0138
1	6^+	6436·8	0·0555	1	6^+	4475·0	0·0474
2	3^-	6521·0	0·0029	0	8^-	4572·9	0·0845
0	8^-	6698·3	0·0249	2	2^+	4654·4	0·0039
1	6^-	6907·9	0·0514	1	6^-	4785·1	0·0543
2	4^+	6914·5	0·0045	0	9^+	4871·2	0·0653
0	9^+	7214·4	0·0105	2	4^-	5196·4	0·0060
3	2^-	7275·1	0·0023	1	7^+	5201·0	0·0662
2	4^-	7313·2	0·0043	0	9^-	5225·7	0·0432
0	9^-	7733·5	0·0028	1	7^-	5425·5	0·0573
1	7^+	7395·9	0·0435	2	4^+	5476·9	0·0066
2	5^+	7715·6	0·0081	0	10^+	5584·6	0·0257
1	7^-	7897·7	0·0322	2	5^-	5732·1	0·0054
2	5^-	8156·6	0·0102	3	2^+	5759·5	0·0018
1	8^+	8411·6	0·0185	1	8^+	5761·5	0·0643
2	6^+	8615·9	0·0118	3	2^-	5776·6	0·0045
1	8^-	8938·3	0·0084	0	10^-	5947·7	0·0130
2	6^-	9090·8	0·0125	2	6^+	6038·6	0·0131
1	9^+	9466·9	0·0017	1	8^-	6105·4	0·0567
2	7^+	9591·5	0·0114	0	11^+	6314·0	0·0051

(*Continued on next page*)

Downloaded At: 17:15 21 January 2011

Table 16. (*continued*).

SiH_3				SiD_3			
v_1	v_2	$\tilde{\nu}$	FC factor	v_1	v_2	$\tilde{\nu}$	FC factor
4	2^+	10123·0	0·0063	2	6^-	6350·8	0·0171
2	8^+	10661·1	0·0021	1	9^+	6457·8	0·0446
3	6^+	10777·3	0·0029	2	7^+	6669·2	0·0231
3	5^-	11311·8	0·0028	1	9^-	6818·7	0·0285
2	9^+	11911·4	0·0015	2	7^-	6992·9	0·0267
				3	5^+	7031·4	0·0013
				1	10^+	7184·4	0·0091
				4	3^-	7324·1	0·0013
				2	8^+	7331·9	0·0267
				1	10^-	7554·8	0·0030
				3	6^+	7591·7	0·0033
				2	8^-	7681·0	0·0158
				3	6^-	7905·3	0·0048
				2	9^+	8125·9	0·0040
				4	4^+	8128·3	0·0073
				3	7^+	8226·1	0·0131
				2	9^-	8413·7	0·0024
				3	7^-	8551·1	0·0126
				3	8^+	8897·4	0·0081
				4	6^+	9135·4	0·0018
				3	8^-	9311·3	0·0045
				4	7^-	9446·7	0·0035
				0	16^+	9848·2	0·0021
				4	9^+	10883·2	0·0013

† Transitions with FC factors of more than 1% of the strongest transition are listed.

Downloaded At: 17:15 21 January 2011

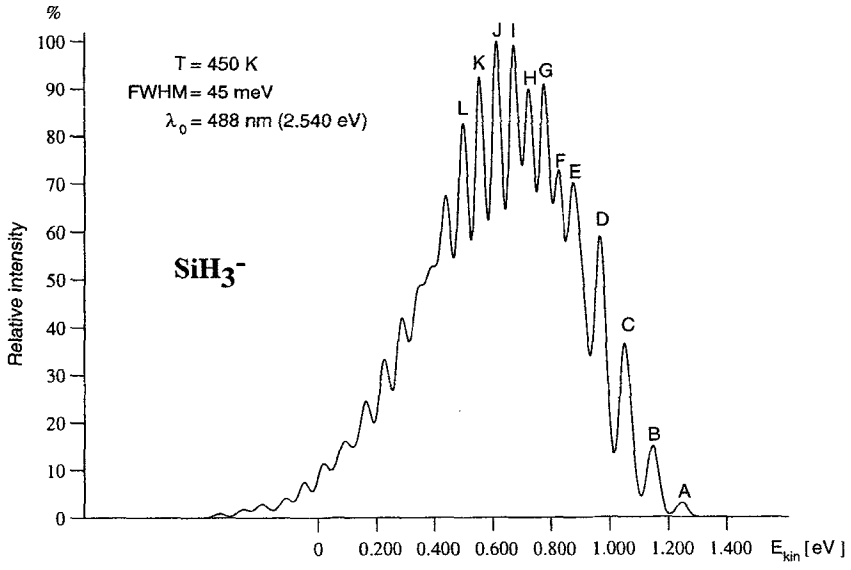

Figure 10. Calculated low-resolution photoelectron spectrum of SiH_3^-.

(see figure 9 of [113]) is very good; practically all essential features are quantitatively reproduced by the present *ab initio* calculations.

Using a large basis of 185 cGTOs the equilibrium electron affinity of SiH_3 was calculated to be 1·307 eV (RCCSD(T)). The adiabatic EA is larger by 0·061 eV. We thus observed very good agreement with the experimental value of 1·406 ± 0·014 eV [113].

7.2. *The photoelectron spectra of CH_2N^- and CD_2N^-*

The photoelectron spectra of CH_2N^- and CD_2N^- were measured by Cowles *et al.* [79] and the electron affinities were determined to be 0·511 ± 0·008 eV and 0·498 ± 0·011 eV, respectively. While the adiabatic peak was found to be dominant in both cases, six additional peaks could be observed for both species. One of them was attributed to a hot band corresponding to excitation of the CH_2 or CD_2 scissoring vibration (ν_3) of the anion. The experimental value for CH_2N^- of about 1370 cm^{-1}, which suffers from a low signal-to-noise ratio, is in fair agreement with a value of 1544 cm^{-1} obtained within the harmonic approximation at the MP2/6-31++G** level [79].

Cowles *et al.* fitted their spectra within the Franck–Condon approximation with a simple model based on three uncoupled oscillators. Under the assumption of no change in the CN equilibrium bond length (R_e) upon ionization which is suggested by the simulation, and an *ab initio* value of 1·27 Å for R_e of the radical [129], they derived r_e (CH) = 1·195 Å and α_e (HCH) = 101° for the anion. These rather unrealistic values are in poor agreement with the MP2 values of the same authors (r_e = 1·139 Å and α_e = 108°) as well as our accurate CCSD(T) results (see table 8). From RCCSD(T) calculations with a basis set of 118 cGTOs we obtain the following changes in the equilibrium geometrical parameters occurring upon electron detachment: $\Delta r_e = -0{\cdot}0466$ Å, $\Delta\alpha_e = 9{\cdot}06°$ and $\Delta R_e = -0{\cdot}0022$ Å. In contrast to the *ab initio* calculations of Cowles *et al.*, but in agreement with experimental findings, we thus obtain almost no change in the CN equilibrium bond length.

We have calculated the vibrational structure of the first band of the PE spectrum of CH_2N^- within a four-dimensional anharmonic model, making use of RCCSD(T) potential energy functions. The calculated spectrum is shown in figure 11; it makes use of the experimental adiabatic electron affinity and uses Gaussian line shapes with a full width at half-maximum (FWHM) of 38 meV as used in the simulation of Cowles *et al.* In agreement with experiment we find the adiabatic peak to be clearly dominating. Peak a is a hot band originating from the first excited state ν_3 ($\sim CH_2$ scissoring vibration) of the anion, which is calculated to have a wavenumber of 1452 cm^{-1}. Peak B corresponds to a transition to the first excited state of the ν_3 vibration of the radical with a wavenumber calculated at 1356 cm^{-1}. This agrees nicely with the matrix infrared value of Jacox [130]. Peak C is composed of transitions to two vibrational states of the radical, ν_1 at 2908 cm^{-1} and $2\nu_3$ at 2705 cm^{-1}. The former is overestimated by our 4D model, which neglects the anharmonic interaction with the b_2 modes (ν_5 and ν_6); we recommend $\nu_1 = 2810 \pm 20$ cm^{-1}. Due to the tiny change in the CN equilibrium bond length no noticeable excitation of the ν_2 vibration ($\sim$CN stretch) is observed or calculated. We predict $\nu_2 = 1635$ cm^{-1}, in poor agreement with the matrix infrared value of 1725·4 cm^{-1} [130]. Since the calculated absolute infrared intensity of this band is only 2·3 km mol^{-1} the experimental value may well be the result of a misassignment as happens rather frequently for free radicals.

The equilibrium electron affinity of CH_2N was calculated by RCCSD(T) using a large basis set of 214 cGTOs (full avqz basis set for C and N, sp(avqz) + d(vqz) for H).

Downloaded At: 17:15 21 January 2011

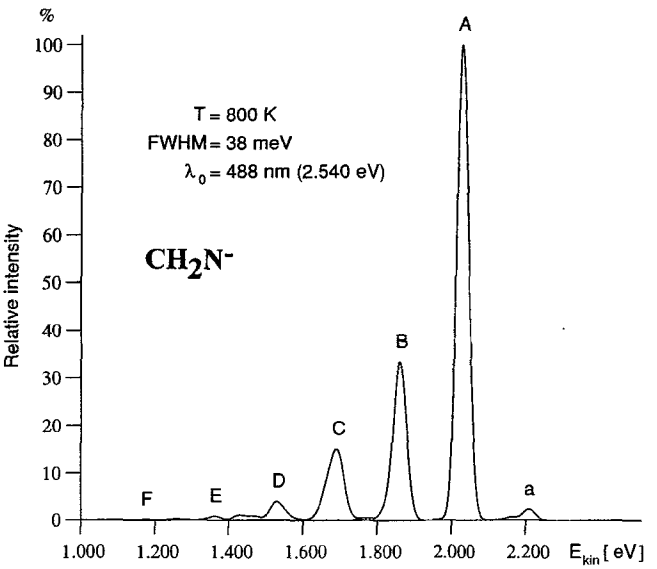

Figure 11. Calculated low-resolution photoelectron spectrum of CH_2N^-.

We obtain $EA_e = 0{\cdot}443$ eV. Adding a zero-point vibrational contribution of 0·0064 eV as obtained from RCCSD(T) calculations with a smaller basis of 118 cGTOs we arrive at $EA_{ad} = 0{\cdot}507$ eV, in excellent agreement with the above experimental value. The differences in the adiabatic electron affinity of CH_2N and CD_2N is calculated to be 0·017 eV. This value should be more accurate than the experimental value of 0·013 eV [79], which has an uncertainty of about 0·01 eV.

7.3. *Electron affinities of linear carbon clusters*

An accurate value of $EA_{ad} = 2{\cdot}853 \pm 0{\cdot}001$ eV was determined for the adiabatic electron affinity of C_5 through threshold photodetachment (ZEKE) spectroscopy [117]. This value refers to the $^2\Pi_{\frac{1}{2}}$ state of the anion. Since spin–orbit splitting among the two components of the vibrational ground state amounts to only 0·003 eV we may well disregard spin–orbit coupling. Since differences in zero-point energies between C_5^- and C_5 are expected to be small (probably not exceeding 0·02 eV) the above adiabatic *EA* should also represent a reasonable estimate for the equilibrium electron affinity (EA_e) which may be directly compared with the results of electronic structure calculations.

The equilibrium geometries of C_5^- ($\tilde{X}^2\Pi_u$) and C_5 ($\tilde{X}^1\Sigma_g^+$) have been discussed in section 4. Here, we make use of the recommended structures. Values for the equilibrium electron affinity from different methods and basis sets are given in table 17. The size of the basis set ranges from 170 to 250 cGTOs. The 195 cGTO set is identical to the 'PVTZ + spd' set of Watts and Bartlett [84]. The present UCCSD and UCCSD(T) values agree with theirs since the slight change in equilibrium geometries (a reduction of 0·007 Å for all bond lengths) is of practically no concern.

The basis set dependence of EA_e, which corresponds to the quantity '*AEA*' of Watts and Bartlett is rather small. Enlargement of the basis from 170 to 250 cGTOs leads to an increase of 0·05 eV for all methods accounting for electron correlation effects. As noted by Watts and Bartlett, UCCSD overestimates EA_e. To a lesser extent this also holds for RCCSD. As is often observed the variant [T] appears to overestimate the

Downloaded At: 17:15 21 January 2011

Table 17. Dependence of the equilibrium electron affinity (EA_e) of C_5 (in eV) on method and basis set†.

Basis	N_{cGTO}	RHF	RCCSD UCCSD	RCCSD[T] UCCSD[T]	RCCSD-T UCCSD-T	RCCSD(T) UCCSD(T)
sp(avtz) + df(vtz)	170	2·175	2·843	2·660	2·700	2·693
			2·902	2·694	2·741	2·729
spd(avtz) + f(vtz)	195	2·174	2·862	2·686	2·726	2·720
			2·921	2·720	2·768	2·756
spd(avtz) + f(vqz)	230	2·174	2·882	2·710	2·750	2·743
			2·941	2·744	2·791	2·779
sp(avqz) + df(vqz)	250	2·173	2·881	2·708	2·747	2·741
			2·941	2·742	2·789	2·777
sp(avqz) + df(avtz)	250	2·174	2·892	2·722	2·762	2·756
			2·952	2·756	2·804	2·792

† Equilibrium geometries employed (see section 4): (*a*) C_5^-: R_{1e} (outer) = 1·2855 Å and R_{2e} (inner) = 1·2996 Å; (*b*) C_5: R_{1e} = 1·2896 Å and R_{2e} = 1·2819 Å [85].

Downloaded At: 17:15 21 January 2011

contribution arising from connected triple substitutions. In comparison with experiment UCCSD-T with the basis described as 'sp(avqz) + df(avtz)' shows the best performance; the calculated EA_e value differs by only 0·05 eV from the experimental EA_{ad} value. Basis set deficiencies of the order of 0·05 eV are not unlikely since functions with higher angular momentum (g, h, ...) may well play a certain role. The differences between the partially restricted and the unrestricted variants of the methods involving connected triples differ by 0·03–0·04 eV. Since the 'R' variants are much less time consuming in an optimal implementation they will certainly have to be preferred for larger systems.

The equilibrium electron affinity of C_6 has been calculated by RCCSD(T) using a basis of 204 cGTO, which corresponds to the 170 cGTO basis for C_5 (see table 17). The calculated equilibrium geometry of C_6^- ($\tilde{X}^2\Pi_u$) has been reported in section 4; that for C_6 ($\tilde{X}^3\Sigma_g^-$) is R_{1e} (outer) = 1·3081 Å, R_{2e} (middle) = 1·2931 Å and R_{3e} (inner) = 1·2808 Å. Again we expect the bond lengths to be too long by about 0·007 Å. The RCCSD(T) value for EA_e is 4·125 eV, in very good agreement with the experimental adiabatic value of 4·185 ± 0·006 eV [118].

Making use of the recommended equilibrium structure for C_8^- ($\tilde{X}^2\Pi_g^-$) from section 4 and the avdz basis set (184 cGTOs) the vertical detachment energy of C_8^- is calculated by RCCSD(T) to be 4·413 eV. It may be compared with the experimental EA_{ad} value of 4·379(6) eV.

8. Polyatomic anions with bound excited electronic states

Most closed-shell negative molecular ions have only one well-bound electronic state. In open-shell anions the situation may be rather different. Good examples are the linear carbon cluster ions C_n^- with an even number of atoms. Already C_2^- has at least two bound excited electronic states (see section 3). Here, we will concentrate on our recent work on C_6^-, C_8^- and C_{10}^-; previous relevant theoretical work on excited states of carbon cluster anions has primarily been published by Adamowicz [119–122] and Bartlett and coworkers [84, 123, 86].

We have carried out large-scale RCCSD(T) calculations for the lowest four doublet states of C_6^-. They are intended to give theoretical support to the tentative assignment of the 608 nm peak found in the neon matrix absorption spectrum of mass-selected

Table 18. Equilibrium bond lengths, equilibrium rotational constants and wave-numbers of totally symmetric stretching vibrations for the four lowest doublet states of C_6^- †.

State	R_{ie} (Å)	R_{me} (Å)	R_{oe} (Å)	B_e MHz	ω_1 (cm^{-1})	ω_2 (cm^{-1})	ω_3 (cm^{-1})
$\tilde{X}^2\Pi_u$	1·2588	1·3318	1·2815	1426·9	2145	1804	637
$\tilde{A}^2\Sigma_g^+$	1·2370	1·3624	1·2470	1430·0	2179	1948	624
$\tilde{B}^2\Sigma_u^+$	1·2361	1·3610	1·2461	1432·5	2179	1952	629
$\tilde{C}^2\Pi_g$	1·2306	1·3837	1·2857	1388·6	2189	1805	599

† RCCSD(T)/204 cGTOs. R_{ie}, R_{me} and R_{oe} are the inner, middle and outer CC equilibrium bond lengths, respectively,

Table 19. Dependence of RCCSD(T) equilibrium excitation energies (T_e) of C_6^- (in eV) on the size of the basis set†.

Basis	N_{cGTO}	$\tilde{A}^2\Sigma_g^+$	$\tilde{B}^2\Sigma_u^+$	$\tilde{C}^2\Pi_g$
avdz	138	1·357	1·406	2·068
sp(avtz) + d(avdz)	162	1·297	1·336	2·098
sp(avtz) + df(vtz)	204	1·316	1·355	2·122
sp(avqz) + d(vqz) + (vtz)	258	1·311	1·350	2·122

† Equilibrium geometries calculated by RCCSD(T)/204 cGTOs, see table 18.

$C_6H_m^-$ [124] to the $^2\Pi_g \leftarrow {}^2\Pi_u$ transition of C_6^- [125]. In previous *ab initio* calculations the vertical excitation energy was predicted to be 2·62 eV (473 nm) and 3·06 eV (405 nm) [120]. Very recent single-excitation CI calculations by Fehér and Maier [125] yielded 2·9 eV (428 nm). Clearly more extended *ab initio* calculations are required to settle the assignment problem.

According to the work of Adamowicz [120] the four lowest doublet states of C_6^- are $\tilde{X}^2\Pi_u$, $\tilde{A}^2\Sigma_g^+$, $\tilde{B}^2\Sigma_u^+$ and $\tilde{C}^2\Pi_g$. Our calculations confirm this ordering which differs from the isoelectronic dicyanoacetylene cation in that the two $^2\Sigma$ states come to lie between the $^2\Pi$ states. Geometry optimization was carried out under the rather well-founded assumption of linear centrosymmetric equilibrium geometries for all four states. A basis set of 204 cGTOs, shortly described as sp(avtz) + df(vtz), was used for this purpose; valence electrons were correlated in the partially spin adapted coupled cluster calculations.

The results are given in table 18. Again, we expect the equilibrium bond lengths to be too long by about 0·007 Å. After having corrected all bond lengths quoted by this increment we arrive at the following predictions for the equilibrium rotational constants: 1442 MHz ($\tilde{X}^2\Pi_u$), 1445 MHz ($\tilde{A}^2\Sigma_g^+$), 1448 MHz ($\tilde{B}^2\Sigma_u^+$) and 1404 MHz ($\tilde{C}^2\Pi_g$). The bond lengths for the $\tilde{A}$ and $\tilde{B}$ states are almost identical. Upon excitation to the $\tilde{C}^2\Pi_g$ state, which according to the work of Fehér and Maier [125] corresponds to the most intense transition, there occurs a substantial contraction of the innermost and a still more pronounced elongation of the middle CC bond.

RCCSD(T) equilibrium excitation energies obtained with different basis sets are listed in table 19. The T_e value for the $\tilde{C}^2\Pi_g$ state shows little basis set dependence. The largest basis of 258 cGTOs yields 2·122 eV, which corresponds to a wavelength of 584 nm. This is clearly in support of the tentative assignment made by Fehér and Maier [125]. A more detailed discussion of the results of our calculations is presented elsewhere [126].

Downloaded At: 17:15 21 January 2011

Table 20. Vertical excitation energies for C_8^- and C_{10}^- (in eV)†.

Species	State	RHF	RCCSD	RCCSD[T]	RCCSD-T	RCCSD(T)
C_8^-	$\tilde{A}^2\Sigma_g^+$	3·556	1·901	1·359	1·403	1·387
	$\tilde{B}^2\Sigma_u^+$	3·560	1·906	1·365	1·409	1·392
	$\tilde{C}^2\Pi_u$	2·613	2·097	1·822	1·839	1·835
C_{10}^-‡	$\tilde{A}^2\Sigma_u^+$	3·441	1·832	1·342	1·378	1·362
	$\tilde{B}^2\Sigma_g^+$	3·442	1·833	1·343	1·379	1·363
	$\tilde{C}^2\Pi_g$	2·162	1·716	1·501	1·508	1·505

† See section 7 for the equilibrium geometries employed. Basis avdz (184 cGTO for C_8^-, 230 cGTO for C_{10}^-).

‡ Contribution of connected triples from 180 cGTO basis (see the text).

No high-level *ab initio* calculations have yet been published for electronically excited states of C_8^- and C_{10}^-. Vertical and some equilibrium excitation energies for C_8^- have been calculated by RHF-SCF and UHF-SCF with a basis set of double-zeta plus polarization (DZP) quality [86]. According to the recent paper of Fehér and Maier [125] the $\Pi_u \leftarrow \Pi_g$ transition of C_8^- may be responsible for the 772 nm absorption observed in matrix isolation experiments.

Calculated vertical excitation energies for C_8^- and C_{10}^- are listed in table 20. They are mainly obtained by the avdz basis set. In the case of C_{10}^- the contribution from connected triple substitutions was calculated from that basis exclusive of d functions with small exponents. RHF yields the incorrect order of the excited states in both cases, with the first excited $^2\Pi$ state lying below the two $^2\Sigma$ states. Throughout the effect of connected triple substitutions is substantial. The RCCSD(T) value for the vertical excitation energy of the $\tilde{C}^2\Pi_u$ state of C_8^- is 1·835 eV. Due to basis set limitations it may be too large by up to about 0·1 eV. The difference between vertical and adiabatic excitation energy is probably of the order of 0·1 eV. We therefore recommend a value of 1·64 ± 0·1 eV for this quantity which again supports the tentative assignment of Fehér and Maier [125].

9. $X^- \cdots CH_3Y$

Cluster anions of type $X^- \ldots CH_3Y$ (X, Y: halogen atoms) are intermediates in nucleophilic substitution (S_N2) reactions. We have investigated three of them at the CEPA-1 level. Wavenumbers and infrared intensities for the totally symmetric vibrations of the three cluster anions are listed in table 21. Since the complex $F^- \cdots CH_3Cl$ is metastable, with a small barrier to arrangement into $Cl^- \cdots CH_3F$, it is not considered here. Anharmonicity effects were variationally taken into account by means of an approximate four-dimensional vibrational Hamiltonian of the form

$$\hat{H}_{vib} = -\frac{\hbar^2}{2}\sum_{i=1}^{4}\frac{\partial^2}{\partial Q_i^2} + V, \tag{5}$$

where Q_i is a totally symmetric normal coordinate and V is the anharmonic potential for totally symmetric modes.

Compared to the free methyl halides the carbon–halogen stretching vibrations in the cluster ions (ν_3) experience substantial red shifts of 154 cm^{-1} ($F^- \cdots CH_3F$, I), 96 cm^{-1} ($Cl^- \cdots CH_3F$, II) and 93 cm^{-1} ($Cl^- \cdots CH_3Cl$, III). In addition, remarkable intensity enhancements occur. A graphical comparison of the complexes with the free methyl halides is made in figure 12.

Downloaded At: 17:15 21 January 2011

Table 21. Harmonic and anharmonic wavenumbers (in cm^{-1}) and infrared intensities (in $km\,mol^{-1}$) for totally symmetric vibrations of cluster anions of type $X^- \ldots CH_3Y$†.

	$F^- \ldots CH_3F$	$Cl^- \ldots CH_3F$	$Cl^- \ldots CH_3Cl$
ω_1	3131 (5)	3121 (18)	3137 (3)
ω_2	1386 (0)	1467 (2)	1347 (15)
ω_3	919 (229)	975 (218)	647 (119)
ω_4	180 (59)	108 (19)	101 (31)
ν_1‡	3101 (4)	3103 (14)	3105 (3)
ν_2	1382 (0)	1457 (2)	1337 (14)
ν_3	897 (229)	954 (220)	636 (122)
ν_4	175 (58)	107 (109)	100 (31)

† CEPA-1 results. Intensity values are given in parentheses.

‡ Due to the neglect of anharmonic interaction with the asymmetric modes the ν_i values are overestimated by about 3%.

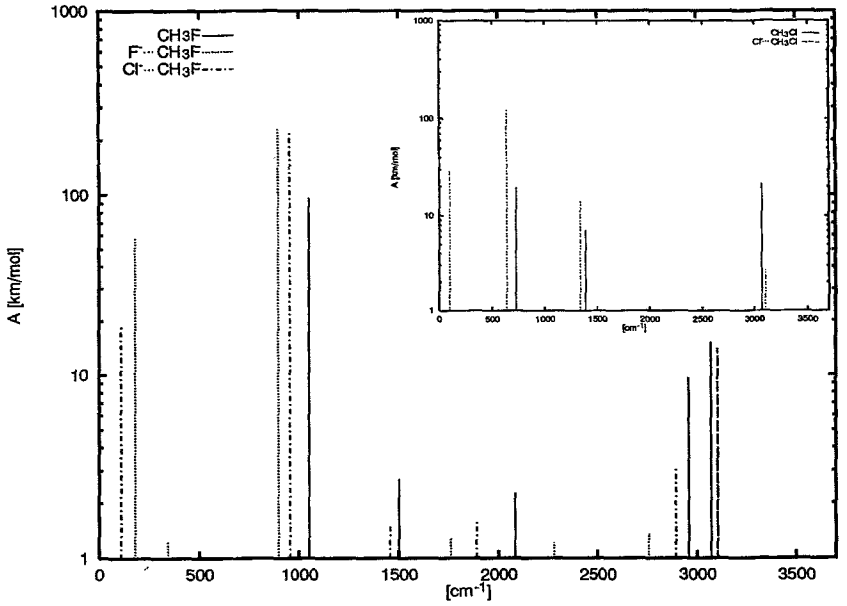

Figure 12. Calculated infrared spectra for complexes of type $X^- \ldots CH_3Y$ and the corresponding methyl halides (only totally symmetric modes considered).

All cluster anions have large dipole moments (in D, with respect to CM system): −6·44 (I), −6·18 (II) and −8·59 (III). They are thus believed to be interesting candidates for forthcoming investigations by millimetre-wave spectroscopy.

10. Conclusions

Due to substantial progress in hardware and programme development, the accuracy of *ab initio* calculations on small negative ions has considerably increased over the past few years. Equilibrium bond lengths can now be calculated with an accuracy of about 0·001 Å and 0·2°, at least for anions with one to four atoms from the first long period. Vibrational wavenumbers may be obtained with an uncertainty of about $10\,cm^{-1}$ (for

Downloaded At: 17:15 21 January 2011

diatomic and triatomic hydrides: about $5\,cm^{-1}$) and calculated vibration–rotation coupling constants and centrifugal distortion constants are accurate to a few per cent. Precise electric dipole moments which could not yet be measured for any negative ion are predicted for some fundamental anions like OH^-, SH^-, CN^-, HCC^-, NH_2^- and NO_2^-. Electron affinities may be obtained with an accuracy of 0·05 eV or better and the vibrational structure of the photoelectron spectra of SiH_3^- and CH_2N^- has been calculated in quantitative agreement with experiment. Structures and spectroscopic properties for three different ionic complexes occurring in S_N2 reactions are calculated as well. The present calculations should be of help to experimentalists in forthcoming high-resolution work on molecular ions. Following a rapid start around 1985, progress in this field has somewhat slowed down. Nevertheless, the authors believe that the prospects for the future are quite good and cooperation between theory and experiment should lead to a substantially increased knowledge on negative ions, with particular emphasis on negative cluster ions.

Acknowledgments

Thanks are due to Professor H.-J. Werner (University of Stuttgart) for providing us with a copy of MOLPRO. Financial support by the Deutsche Forschungsgemeinschaft (through SFB 357, grant Bo481/6-1,2 and grant Ml7/1-1) and the Fonds der Chemischen Industrie is gratefully acknowledged. We thank the Gesellschaft für wissenschaftliche Datenverarbeitung at Göttingen and the Regionales Hochschulrechenzentrum at Hannover for providing computation time.

Downloaded At: 17:15 21 January 2011

Note added in proof

After submission of this paper an excellent review article by Kalcher and Sax appeared (J. Kalcher and A. F. Sax, 1994, *Chem. Rev.*, **94,** 2291) which concentrates mainly on energetic aspects of anions, dianions and higher charged anions.

References

[1] HERZBERG, G., and LAGERQVIST, A., 1968, *Can. J. Phys.*, **46,** 2363.
[2] JONES, P. L., MEAD, R. D., KOHLER, B. E., ROSNER, S. D., and LINEBERGER, W. C., 1980, *J. chem. Phys.*, **73,** 4419.
[3] SCHULZ, P. A., MEAD, R. D., JONES, P. L., and LINEBERGER, W. C., 1982, *J. chem. Phys.*, **77,** 1153.
[4] NEUMARK, D. M., LYKKE, K. R., ANDERSEN, T., and LINEBERGER, W. C., 1985, *Phys. Rev.* A, **32,** 1890.
[5] MILLER, H. C., HARDWICK, J. L., and FARLEY, J. W., 1989, *J. molec. Spectrosc.*, **134,** 329.
[6] LYKKE, K. R., MEAD, R. D., and LINEBERGER, W. C., 1984, *Phys. Rev. Lett.*, **52,** 2221.
[7] MEAD, R. D., LYKKE, K. R., LINEBERGER, W. C., MARKS, J., and BRAUMAN, J. I., 1984, *J. chem. Phys.*, **81,** 4883.
[8] LYKKE, K. R., NEUMARK, D. M., ANDERSEN, T., TRAPA, V. J., and LINEBERGER, W. C., 1987, *J. chem. Phys.*, **87,** 6842.
[9] MARKS, J., BRAUMAN, J. I., MEAD, R. D., LYKKE, K. R., and LINEBERGER, W. C, 1988, *J. chem. Phys.*, **88,** 6785.
[10] YOKOYAMA, K., private communication, 1994.
[11] GUDEMAN, C. S., and SAYKALLY, R. J., 1984, *Ann. Rev. Phys. Chem.*, **35,** 387, and references therein.
[12] OWRUTSKY, J., ROSENBAUM, N., TACK, L., and SAYKALLY, R. J., 1985, *J. chem. Phys.*, **83,** 5338.
[13] ROSENBAUM, N. H., OWRUTSKY, J. C., TACK, L. M., and SAYKALLY, R. J., 1986, *J. chem. Phys.*, **84,** 5308.
[14] TACK, L. M., ROSENBAUM, N. J., OWRUTSKY, J. C., and SAYKALLY, R. J., 1986, *J. chem. Phys.*, **84,** 8056.

[15] TACK, L. M., ROSENBAUM, N. H., OWRUTSKY, J. C., and SAYKALLY, R. J., 1986, *J. chem. Phys.*, **85,** 4222.
[16] GRUEBELE, M., POLAK, M., and SAYKALLY, R. J., 1987, *J. chem. Phys.*, **86,** 1698.
[17] POLAK, M., GRUEBELE, M., and SAYKALLY, R. J., 1987, *J. Am. Chem. Soc.*, **109,** 2884.
[18] POLAK, M., GRUEBELE, M., PENG, G. S., and SAYKALLY, R. J., 1988, *J. chem. Phys.*, **89,** 110.
[19] GRUEBELE, M., POLAK, M., and SAYKALLY, R. J., 1987, *J. chem. Phys.*, **86,** 6631.
[20] POLAK, M., GRUEBELE, M., and SAYKALLY, R. J., 1987, *J. chem. Phys.*, **87,** 3352.
[21] KAWAGUCHI, K., and HIROTA, E., 1986, *J. chem. Phys.*, **84,** 2953.
[22] KAWAGUCHI, K., and HIROTA, E., 1987, *J. chem. Phys.*, **87,** 6838.
[23] KAWAGUCHI, K., 1988, *J. chem. Phys.*, **88,** 4186.
[24] GRUEBELE, M., POLAK, M., and SAYKALLY, R. J., 1987, *J. chem. Phys.*, **87,** 1448.
[25] BOTSCHWINA, P., 1988, *J. chem. Soc. Faraday Trans.* II, **84,** 1561.
[26] BOTSCHWINA, P., 1989, *Ion and Cluster Ion Spectroscopy and Structure*, edited by J. P. Maier (Amsterdam: Elsevier).
[27] ERVIN, K. M., and LINEBERGER, W. C., 1991, *J. chem. Phys.*, **95,** 1167.
[28] BATES, D. R., 1991, *Adv. atom molec. optic. Phys.*, **27,** 1.
[29] WERNER, H.-J., and KNOWLES, P., 1988, *J. chem. Phys.*, **89,** 5803, and references therein.
[30] ROOS, B. O., TAYLOR, P. R., and SIEGBAHN, P. E. M., 1980, *Chem. Phys.*, **48,** 157.
[31] ROOS, B. O., 1987, *Adv. chem. Phys.*, **69,** 399.
[32] KRISHNAN, R., FRISCH, M. J., and POPLE, J. A., 1980, *J. chem. Phys.*, **72,** 4244, and references therein.
[33] BARTLETT, R. J., 1989, *J. chem. Phys.*, **93,** 1697.
[34] KÜMMEL, H., 1991, *Theor. chim. Acta*, **80,** 81.
[35] ČÍŽEK, J., 1991, *Theor. chim. Acta*, **80,** 91.
[36] RENDELL, A. P., LEE, T. J., and TAYLOR, P. R., 1990, *J. chem. Phys.*, **92,** 7050.
[37] LEE, T. J., and SCUSERIA, G. E., 1990, *J. chem. Phys.*, **93,** 489.
[38] LEE, T. J., RENDELL, A. P., and TAYLOR, P. R., 1990, *J. phys. Chem.*, **94,** 5468.
[39] SCUSERIA, G. E., and LEE, T. J., 1990, *J. chem. Phys.*, **93,** 5851.
[40] RAGHAVACHARI, K., TRUCKS, G. W., POPLE, J. A., and HEAD-GORDON, M., 1989, *Chem. Phys. Lett.*, **157,** 479.
[41] RITTBY, M., and BARTLETT, R. J., 1988, *J. phys. Chem.*, **92,** 3033.
[42] SCUSERIA, G., 1991, *Chem. Phys. Lett.*, **176,** 27.
[43] JANSSEN, C., and SCHAEFER III, H. F., 1991, *Theor. Chim. Acta*, **79,** 1.
[44] JAYATILAKA, D., and LEE, T. J., 1992, *Chem. Phys. Lett.*, **199,** 211.
[45] JAYATILAKA, D., and LEE, T. J., 1993, *J. chem. Phys.*, **98,** 9734.
[46] WATTS, J. D., and BARTLETT, R. J., 1990, *J. chem. Phys.*, **93,** 6104.
[47] GAUSS, J., LAUDERDALE, W. J., STANTON, J. F., WATTS, J. D., and BARTLETT, R. J., 1991, *Chem. Phys. Lett.*, **182,** 207.
[48] WATTS, J. D., GAUSS, J., and BARTLETT, R. J., 1993, *J. chem. Phys.*, **98,** 8718.
[49] KNOWLES, P. J., HAMPEL, C., and WERNER, H.-J., 1993, *J. chem. Phys.*, **99,** 5219.
[50] DEEGAN, M. J. O., and KNOWLES, P. J., 1994, *Chem. Phys. Lett.*, **227,** 321.
[51] MEYER, W., 1971, *Int. J. quant. Chem. Symp.*, **5,** 341.
[52] MEYER, W., 1973, *J. chem. Phys.*, **58,** 1017.
[53] MØLLER, C., and PLESSET, M. S., 1934, *Phys. Rev.* A, **46,** 618.
[54] POPLE, J. A., BINKLEY, J. S., and SEEGER, R., 1976, *Int. J. quant. Chem. Symp.*, **10,** 1.
[55] BOTSCHWINA, P., HORN, M., FLÜGGE, J., and SEEGER, S., 1993, *J. Chem. Soc. Faraday Trans.*, **89,** 2219.
[56] BOTSCHWINA, P., OSWALD, M., FLÜGGE, J., HEYL, Ä., and OSWALD, R., 1993, *Chem. Phys. Lett.*, **209,** 117.
[57] ROSMUS, P., and MEYER, W., 1978, *J. chem. Phys.*, **69,** 2745.
[58] MOLPRO is a package of *ab initio* programmes by H.-J. Werner and P. J. Knowles, with contributions of J. Almlöf, R. D. Amos, M. J. O. Deegan, S. Elbert, C. Hampel, W. Meyer, K. A. Peterson, R. M. Pitzer, A. J. Stone and P. R. Taylor.
[59] KENDALL, R. A., DUNNING, T. H., and HARRISON, R. J., 1992, *J. chem. Phys.*, **96,** 6796.
[60] SENEKOWITSCH, J., WERNER, H.-J., ROSMUS, P., REINSCH, E.-A., and O'NEIL, S. V., 1985, *J. chem. Phys.*, **83,** 4661.
[61] NEUMARK, D. M., LYKKE, K. R., ANDERSEN, T., and LINEBERGER, W. C., 1985, *J. chem. Phys.*, **83,** 4364.
[62] AL-ZA'AL, M., MILLER, H. C., and FARLEY, J. W., 1986, *Chem. Phys. Lett.*, **131,** 56.

Downloaded At: 17:15 21 January 2011

[63] AL-ZA'AL, M., MILLER, H. C., and FARLEY, J. W., 1987, *Phys. Rev.* A, **35,** 1099.
[64] MILLER, H. C., and FARLEY, J. W., 1987, *J. chem. Phys.*, **86,** 1167.
[65] MÄNZ, U., ZILCH, A., ROSMUS, P., and WERNER, H.-J., 1986, *J. chem. Phys.*, **84,** 5037.
[66] MLADENOVIĆ, M., SCHMATZ, S., and BOTSCHWINA, P., 1994, *J. chem. Phys.*, **101,** 5891.
[67] BOTSCHWINA, P., 1985, *Chem. Phys. Lett.*, **114,** 58.
[68] PETERSON, K. A., and WOODS, R. C., 1987, *J. chem. Phys.*, **87,** 4409.
[69] SHERMAN, W. F., and WILKINSON, G. R., 1973, *Vibrational Spectroscopy of Trapped Species*, edited by H. E. Hallam (London, Wiley).
[70] FORNEY, D., THOMPSON, W. E., and JACOX, M. E., 1992, *J. chem. Phys.*, **97,** 1664.
[71] BRADFORTH, S. E., KIM, E. H., ARNOLD, D. W., and NEUMARK, D. M., 1993, *J. chem. Phys.*, **98,** 800.
[72] SCUSERIA, G. E., MILLER, M. D., JENSEN, F., and GEERTSEN, J., 1991, *J. chem. Phys.*, **94,** 6660.
[73] LAUGHLIN, K. B., BLAKE, G. A., COHEN, R. C., HOVDE, D. C., and SAYKALLY, R. J., 1987, *Phys. Rev. Lett.*, **58,** 996.
[74] HAVENITH, M., ZWART, E., MEERTS, L., and TERMEULEN, J. J., 1990, *J. chem. Phys.*, **93,** 8446.
[75] GRANER, G., 1992, *Accurate molecular structures*, edited by A. Domenicano and I. Hargittai (Oxford University Press).
[76] BOTSCHWINA, P., HORN, M., SEEGER, S., and FLÜGGE, J., 1993, *Molec. Phys.*, **78,** 191.
[77] BOTSCHWINA, P., 1986, *J. chem. Phys.*, **85,** 4591.
[78] BOTSCHWINA, P., SEEGER, S., and FLÜGGE, J., 1993, *J. chem. Phys.*, **99,** 8349; *Ibid.*, **117,** 173.
[79] COWLES, D. C., TRAVERS, M. J., FRUEH, J. L., and ELLISON, G. B., 1991, *J. chem. Phys.*, **94,** 3517.
[80] LOHR, L. L., 1985, *J. phys. Chem.*, **89,** 3465.
[81] KOCH, W., and FRENKING, G., 1987, *J. chem. Phys.*, **91,** 49.
[82] DUNNING, T. H., 1989, *Chem. Phys.*, **90,** 1007.
[83] TANAKA, Y., and MACHIDA, K., 1977, *J. molec. Spectrosc.*, **64,** 429.
[84] WATTS, J. D., and BARTLETT, R. J., 1994, *J. chem. Phys.*, **101,** 409.
[85] BOTSCHWINA, P., 1994, *J. chem. Phys.*, **101,** 853.
[86] WATTS, J. D., and BARTLETT, R. J., 1992, *J. chem. Phys.*, **97,** 3445.
[87] BOTSCHWINA, P., 1986, *J. molec. Spectrosc.*, **117,** 173.
[88] SWANTON, D. J., BACSKAY, G. B., and HUSH, N. S., 1986, *Chem. Phys.*, **107,** 25.
[89] SUZER, S., and ANDREWS, L., 1988, *J. chem. Phys.*, **89,** 5347.
[90] BAČIĆ, Z., and LIGHT, J. C., 1989, *Ann. Rev. Phys. Chem.*, **40,** 469.
[91] MLADENOVIĆ, M., and BAČIĆ, Z., 1990, *J. chem. Phys.*, **93,** 3039.
[92] BAČIĆ, Z., 1991, *J. chem. Phys.*, **95,** 3456.
[93] FEHSENFELD, F. C., and FERGUSON, E. E., 1974, *J. chem. Phys.*, **61,** 3181.
[94] ERVIN, K. M., HO, J., and LINEBERGER, W. C., 1988, *J. phys. Chem.*, **92,** 5405.
[95] MILLIGAN, D. E., JACOX, M. E., and GULILLORY, W. A., 1970, *J. chem. Phys.*, **52,** 3864.
[96] MILLIGAN, D. E., and JACOX, M. E., 1971, *J. chem. Phys.*, **55,** 3404.
[97] FORNEY, D., THOMPSON, W. E., and JACOX, M. E., 1993, *J. chem. Phys.*, **99,** 7393.
[98] PETERSON, K. A., MAYRHOFER, R. C., SIBERT III, E. L., and WOODS, R. C., 1991, *J. chem. Phys.*, **94,** 414.
[99] OAKES, J. M., HARDING, L. B., and ELLISON, G. B., 1985, *J. chem. Phys.*, **83,** 5400.
[100] VAZQUEZ, G. J., BUENKER, R. J., and PEYERIMHOFF, S. D., 1989, *Chem. Phys.*, **129,** 405.
[101] SEBALD, P., 1990, Dissertation, Kaiserslautern.
[102] BOTSCHWINA, P., and SEBALD, P., 1991, *Fundamentals of Gas Phase Ion Chemistry*, edited by K. R. Jennings (Dordrecht: Kluwer).
[103] BOTSCHWINA, P., 1986, *J. chem. Phys.*, **85,** 4591.
[104] SENEKOWITSCH, J., and ROSMUS, P., 1987, *J. chem. Phys.*, **86,** 6329.
[105] BOTSCHWINA, P., SEBALD, P., and BURMEISTER, R., 1988, *J. chem. Phys.*, **88,** 5246.
[106] BOTSCHWINA, P., 1984, Habilitationsschrift, Kaiserslautern.
[107] LEE, T. J., and SCHAEFER III, H. F., 1985, *J. chem. Phys.*, **83,** 1784.
[108] BOTSCHWINA, P., 1982, *Chem. Phys.*, **68,** 41.
[109] BOTSCHWINA, P., FLESCH, J., and MEYER, W., 1983, *Chem. Phys.*, **81,** 73.
[110] BOTSCHWINA, P., SCHULZ, B., HORN, M., and MATUSCHEWSKI, M., 1995, *Chem. Phys.*, **190,** 345.

Downloaded At: 17:15 21 January 2011

[111] KHILIFI, M., RAULIN, F., ARIE, E., and GRANER, G., 1990, *J. molec. Spectrosc.*, **143,** 209.
[112] UYEMURA, M., and MAEDA, S., 1974, *Bull. Chem. Soc. Jpn.*, **47,** 2930.
[113] NIMLOS, M. R., and ELLISON, C. B., 1986, *J. Am. Chem. Soc.*, **108,** 6522.
[114] BOTSCHWINA, P., 1983, *Chem. Phys.*, **74,** 321.
[115] BOTSCHWINA, P., ROSMUS, P., and REINSCH, E. A., 1983, *Chem. Phys. Lett.*, **102,** 299.
[116] HORN, M., and BOTSCHWINA, P., 1994, *Chem. Phys. Lett.*, **228,** 259.
[117] KITSOPOULOS, T. N., CHICK, C. J., ZHAO, Y., and NEUMARK, D. M., 1991, *J. chem. Phys.*, **95,** 5479.
[118] ARNOLD, D. W., BRADFORTH, S. E., KITSOPOULOS, T. N., and NEUMARK, D. M., 1991, *J. chem. Phys.*, **95,** 8753.
[119] ADAMOWICZ, L., 1991, *Chem. Phys. Lett.*, **180,** 466.
[120] ADAMOWICZ, L., 1991, *Chem. Phys. Lett.*, **182,** 45.
[121] ADAMOWICZ, L., 1991, *J. chem. Phys.*, **94,** 1241.
[122] ADAMOWICZ, L., 1991, *J. chem. Phys.*, **95,** 8669.
[123] WATTS, J. D., CERNUSAK, I., and BARTLETT, R. J., 1991, *Chem. Phys. Lett.*, **178,** 259.
[124] FULARA, J., LESSEN, D., FREIVOGEL, P., and MAIER, J. P., 1993, *Nature*, **366,** 439.
[125] FEHÉR, M., and MAIER, J. P., 1994, *Chem. Phys. Lett.*, **227,** 371.
[126] SCHMATZ, S., and BOTSCHWINA, P., 1995, *Chem. Phys. Lett.*, **235,** 5.
[127] WERNER, H.-J., ROSMUS, P., and REINSCH, E.-A., 1983, *J. chem. Phys.*, **79,** 905.
[128] SMITH JR, D. F., and YORK, R. J., 1974, *J. chem. Phys.*, **61,** 5028.
[129] BAIR, R. A., and DUNNING JR, T. H., 1985, *J. chem. Phys.*, **82,** 2280.
[130] JACOX, M. E., 1987, *J. phys. Chem.*, **91,** 6595.
[131] ROSMUS, P., and WERNER, H.-J., 1984, *J. chem. Phys.*, **80,** 5085.
[132] REHFUSS, B. D., LIU, D.-J., DINELLI, B. M., JAGOD, M.-F., HO, W. C., CROFTON, M. W., and OKA, T., 1988, *J. chem. Phys.*, **89,** 129.
[133] WATTS, J. D., and BARTLETT, R. J., 1992, *J. Chem. Phys.*, **96,** 6073.
[134] ZEITZ, M., PEYERIMHOFF, S. D., and BUENKER, R. J., 1979, *Chem. Phys. Lett.*, **64,** 243.
[135] MEAD, R. D., HEFTER, U., SCHULZ, P. A., and LINEBERGER, W. C., 1985, *J. Chem. Phys.*, **82,** 1723.

Downloaded At: 17:15 21 January 2011